

Exploring the nucleus in the context of low-energy QCD

Dario Vretenar¹ and Wolfram Weise²

¹ Physics Department, Faculty of Science, University of Zagreb, 10 000 Zagreb, Croatia [vretenar@phy.hr]

² ECT*, I-38050 Villazzano (Trento), Italy and Physik-Department, Technische Universität München, D-85747 Garching, Germany [weise@ect.it]

Summary. These lecture notes address a central problem of theoretical nuclear physics: how to establish a relationship between *low-energy, non-perturbative QCD* and *nuclear phenomenology* which includes both nuclear matter and finite nuclei. We develop a microscopic covariant description of nuclear many-body dynamics constrained by chiral symmetry and in-medium QCD sum rules. A relativistic point-coupling model is derived, based on an effective Lagrangian with density-dependent contact interactions between nucleons. These interactions are constructed from chiral one- and two-pion exchange, combined with the large isoscalar nucleon self-energies that arise through changes in the quark condensate and the quark density at finite baryon density. Nuclear binding and saturation are almost completely generated by chiral (two-pion exchange) fluctuations in combination with Pauli effects, whereas strong scalar and vector fields of about equal magnitude and opposite sign, induced by changes of the QCD vacuum in the presence of baryonic matter, generate the large effective spin-orbit potential in finite nuclei. Promising results are found for the nuclear matter equation of state and for the bulk and single-nucleon properties of finite nuclei.

1 Introduction

The physics based on Quantum Chromodynamics (QCD), the fundamental theory of interacting quarks and gluons, is undoubtedly one of the most fascinating fields of modern science. It covers an enormously wide spectrum of phenomena, ranging from hadrons and nuclei to matter under extreme conditions of temperature and density. How the basic quark constituents and gluon fields arrange themselves to form nucleons and mesons, and how these localized clusters of confined quarks and gluons interact collectively in nuclei: these are key questions of nuclear physics.

At very short distance scales, $r < 0.1$ fm, corresponding to momentum transfers above several GeV/c which probe space-time intervals deep inside the nucleon, QCD is a theory of weakly interacting, pointlike quarks and gluons. The rules for their dynamics are set by local gauge invariance under $SU(3)_{color}$. This is the area of perturbative QCD, an active field of research all by itself but with little direct impact on the understanding of nuclei in which the relevant length scale (e.g. the average separation between nucleons) is typically more than twice the size of the individual nucleon. At such large distance scales, $r > 1$ fm, QCD is realised as a theory of pions coupled to nucleons (and possibly other heavy, almost static

hadrons). Their dynamics is governed by an approximate symmetry of QCD: *Chiral Symmetry*, and its spontaneous breakdown at low energy.

The non-linear dynamics of gluons and their strong interactions with quarks imply a complex structure of the QCD ground state (or "vacuum"): it hosts strong condensates of quark-antiquark pairs and gluons, an entirely non-perturbative phenomenon. The quark condensate $\langle \bar{q}q \rangle$, i.e. the ground state expectation value of the scalar quark density, plays a particularly important role as an order parameter of spontaneously broken chiral symmetry. Hadrons, as well as nuclei, are excitations built on this condensed ground state. Changes of the condensate structure of the QCD vacuum in the presence of baryonic matter are a source of strong fields experienced by the nucleons. The nuclear dynamics governed by these strong fields, together with the pion-exchange forces that determine the nucleon-nucleon interaction at long and intermediate distances, will be important elements in our discussion.

Our framework is the effective field theory that represents low-energy QCD with the lightest (u and d) quarks. This theory is written in terms of an effective Lagrangian constructed according to the symmetries and symmetry breaking patterns of QCD. Identifying the relevant, active degrees of freedom at low energy is the first important step in this approach. Nuclei are aggregates living in the low-temperature (hadronic) sector of the QCD phase diagram, where quarks and gluons are confined in color singlet mesons and baryons. At the energy and momentum scales characteristic of nuclei, only the states of lowest mass in the meson and baryon spectrum are expected to be "active": pions and nucleons. Their quark-gluon substructure and detailed short-distance dynamics are not resolved at nuclear scales. In the effective field theory the substructures of pions and nucleons are encoded through measured structure constants and through contact interactions with parameters to be determined empirically. The effective field theory approach does have predictive power, in the sense that there exists a guiding (symmetry) principle for constructing an ordered hierarchy of terms in the effective Lagrangian. The parameters of the leading terms are controlled or constrained by measurements of independent subprocesses such as pion-nucleon scattering.

Nuclear phenomenology has, of course, a long history and a rich empirical background that we can build on. Concepts such as density functional theory and effective field theory are at the basis of many successful nuclear structure models. Quantum Hadrodynamics (QHD), in particular, represents a class of Lorentz-covariant, meson-nucleon or point-coupling models of nuclear dynamics, that have been used successfully in studies of a variety of nuclear phenomena [1]. Models based on the relativistic mean-field (RMF) approximation of QHD have been applied to describe various properties of spherical and deformed nuclei all over the periodic table [2].

Pions, as Goldstone bosons of spontaneously broken chiral symmetry, are well known to be important ingredients in nuclear systems [3]. The behavior of the nucleon-nucleon interaction at long and intermediate distances is determined by one- and two-pion exchange processes. Ab-initio many-body calculations of nuclear matter and light nuclei [4] strongly emphasize the crucial role played by the pion-exchange tensor force. Nevertheless, pions are usually not included as explicit degrees of freedom in QHD-type calculations. The most successful QHD models are so far purely phenomenological. Effects of two-pion exchange are treated only implicitly through an ad-hoc scalar-isoscalar mean field.

The successes of relativistic nuclear mean-field approaches have been attributed primarily to the large Lorentz scalar and four-vector nucleon self-energies which are at the basis of all QHD models [5]. There is substantial (though indirect) evidence, in particular from nuclear matter saturation and abnormally large spin-orbit splittings in nuclei, that the magnitude of each of the scalar and vector mean fields experienced by nucleons in the nuclear interior is of the order of several hundred MeV. Studies based on finite-density QCD sum rules have shown how such large scalar and vector nucleon self-energies can arise naturally from the in-medium changes of the scalar quark condensate and the quark density [6, 7, 8]. In most applications of QHD models to finite nuclei, however, the interactions generating these large nucleon self-energies have been treated in a purely phenomenological way. In some models they arise from the exchange of "sigma" and "omega" bosons with adjustable coupling strengths. The physical meaning of such assumed ad-hoc mechanisms may be seen in different perspective when exploring their basic QCD connection.

These lecture notes describe and summarize recent developments based on the following conjectures that are believed to establish links between low-energy QCD, its symmetry breaking pattern, and the nuclear many-body problem:

- The nuclear ground state is characterized by large scalar and vector fields of approximately equal magnitude and opposite sign. These fields have their origin in the in-medium changes of the scalar quark condensate (the chiral condensate) and of the quark density.
- Nuclear binding and saturation arise predominantly from chiral (pionic) fluctuations (reminiscent of van der Waals forces) in combination with Pauli blocking effects, superimposed on the condensate background fields and calculated according to the rules of in-medium chiral perturbation theory.

We begin by briefly summarizing important aspects of low-energy QCD and chiral symmetry inasmuch as they are relevant to our theme. Elements of in-medium chiral perturbation theory and results from QCD sum rules at finite density are also described. We then proceed by studying nuclear matter and nucleon self-energies in the context of chiral dynamics and with constraints from the expected changes of condensates at finite baryon density. In the next step, these features are translated into an equivalent relativistic point-coupling model with density dependent coupling strengths. This model is used to calculate a variety of bulk and single particle properties of finite nuclei, from ^{16}O to ^{90}Zr . We conclude with an outlook and a discussion of further steps that are still ahead.

Much of the material and many of the results presented here have appeared in recent publications [9, 10, 11, 12, 13]. A presentation of the general framework can be found in previous lecture notes [14]. Introductory surveys on basic QCD notions related to our subject are given in several chapters of ref. [15].

2 Low-energy QCD

2.1 Chiral symmetry

Our framework is QCD in the sector of the lightest (u, d) quarks. They form a flavour $N_f = 2$ (isospin) doublet with "bare" quark masses of less than 10 MeV. The flavour (and colour) components of the quarks are collected in the Dirac fields $\psi(x) = (u(x), d(x))^T$. The QCD Lagrangian,

$$\mathcal{L}_{QCD} = \bar{\psi}(i\gamma_\mu D^\mu - m)\psi - \frac{1}{2}\text{Tr}(G_{\mu\nu}G^{\mu\nu}), \quad (1)$$

involves the $SU(3)_{color}$ gauge covariant derivative D^μ and the gluonic field tensor $G^{\mu\nu} = (i/g)[D^\mu, D^\nu]$. The 2×2 matrix $m = \text{diag}(m_u, m_d)$ contains the light quark masses. The strange quark is more than an order of magnitude heavier ($m_s \sim 150$ MeV), but still sometimes considered "light" on the typical GeV scales of strong interaction physics. It will nevertheless be ignored in the present discussion, together with the heavy quarks ($Q = c, b$ and t).

Consider QCD in the limit of massless quarks, setting $m = 0$ in Eq.(1). In this limit, the QCD Lagrangian has a global symmetry related to the conserved right- or left-handedness (chirality) of zero mass spin 1/2 particles. Introducing right- and left-handed quark fields,

$$\psi_{R,L} = \frac{1}{2}(1 \pm \gamma_5)\psi, \quad (2)$$

we observe that separate global unitary transformations

$$\psi_R \rightarrow \exp[i\theta_R^a \frac{\tau_a}{2}] \psi_R, \quad \psi_L \rightarrow \exp[i\theta_L^a \frac{\tau_a}{2}] \psi_L, \quad (3)$$

with $\tau_a (a = 1, 2, 3)$ the generators of (isospin) $SU(2)$, leave \mathcal{L}_{QCD} invariant in the limit $m \rightarrow 0$. This is the chiral $SU(2)_R \times SU(2)_L$ symmetry of QCD. It implies six conserved Noether currents, $J_{R,a}^\mu = \bar{\psi}_R \gamma^\mu \frac{\tau_a}{2} \psi_R$ and $J_{L,a}^\mu = \bar{\psi}_L \gamma^\mu \frac{\tau_a}{2} \psi_L$, with $\partial_\mu J_R^\mu = \partial_\mu J_L^\mu = 0$. It is common to introduce the vector and axial currents,

$$V_a^\mu = J_{R,a}^\mu + J_{L,a}^\mu = \bar{\psi} \gamma^\mu \frac{\tau_a}{2} \psi, \quad A_a^\mu(x) = J_{R,a}^\mu - J_{L,a}^\mu = \bar{\psi} \gamma^\mu \gamma_5 \frac{\tau_a}{2} \psi. \quad (4)$$

Their corresponding charges,

$$Q_a^V = \int d^3x \psi^\dagger(x) \frac{\tau_a}{2} \psi(x), \quad Q_a^A = \int d^3x \psi^\dagger(x) \gamma_5 \frac{\tau_a}{2} \psi(x), \quad (5)$$

are, likewise, generators of $SU(2) \times SU(2)$.

2.2 Spontaneous chiral symmetry breaking

There is evidence from hadron spectroscopy that the chiral $SU(2) \times SU(2)$ symmetry of the QCD Lagrangian (1) with $m = 0$ is spontaneously broken: for dynamical reasons of non-perturbative origin, the ground state (vacuum) of QCD has lost part of the symmetry of the Lagrangian. It is symmetric only under the subgroup $SU(2)_V$ generated by the vector charges Q^V . This is the well-known isospin symmetry seen in spectroscopy and dynamics.

If the ground state of QCD were symmetric under chiral $SU(2) \times SU(2)$, both vector and axial charge operators would annihilate the vacuum: $Q_a^V|0\rangle = Q_a^A|0\rangle = 0$. This is the Wigner-Weyl realisation of chiral symmetry with a "trivial" vacuum. It would imply the systematic appearance of parity doublets in the hadron spectrum. For example, correlation functions of vector and axial vector currents should be identical, i. e. $\langle 0|V^\mu V^\nu|0\rangle = \langle 0|A^\mu A^\nu|0\rangle$. Consequently, the spectra of vector ($J^\pi = 1^-$) and axial vector ($J^\pi = 1^+$) mesonic excitations should also be identical. This degeneracy is not seen in nature: the ρ meson mass ($m_\rho \simeq 0.77$ GeV) is well separated from that of the a_1 meson ($m_{a_1} \simeq 1.23$ GeV). Likewise, the light pseudoscalar ($J^\pi = 0^-$) mesons have masses much lower than the lightest scalar ($J^\pi = 0^+$) mesons.

One must conclude $Q_a^A|0\rangle \neq 0$, that is, chiral symmetry is spontaneously broken down to isospin: $SU(2)_R \times SU(2)_L \rightarrow SU(2)_V$. This is the Nambu-Goldstone realisation of chiral symmetry. Goldstone's theorem says that a spontaneously broken global symmetry implies the existence of a massless boson (the Goldstone boson). Let us give a sketch of this theorem. If $Q_a^A|0\rangle \neq 0$, there must be a physical state generated by the axial charge, $|\phi_a\rangle = Q_a^A|0\rangle$, which is energetically degenerate with the vacuum. Let H_0 be the QCD Hamiltonian (with massless quarks) which commutes with the axial charge. Setting the ground state energy equal to zero for convenience, we have $H_0|\phi_a\rangle = Q_a^A H_0|0\rangle = 0$. Evidently $|\phi_a\rangle$ represents three massless pseudoscalar bosons (for $N_f = 2$). They are identified with the pions.

2.3 The chiral condensate

Spontaneous chiral symmetry breaking goes together with a qualitative rearrangement of the vacuum, an entirely non-perturbative phenomenon. The ground state is now populated by scalar quark-antiquark pairs. The corresponding ground state expectation value $\langle 0|\bar{\psi}\psi|0\rangle$ is called the chiral (or quark) condensate. We frequently use the notation

$$\langle \bar{\psi}\psi \rangle = \langle \bar{u}u \rangle + \langle \bar{d}d \rangle . \quad (6)$$

The precise definition of the chiral condensate is:

$$\langle \bar{\psi}\psi \rangle = -iTr \lim_{y \rightarrow x^+} S_F(x, y) \quad (7)$$

with the full quark propagator, $S_F(x, y) = -i\langle 0|\mathcal{T}\psi(x)\bar{\psi}(y)|0\rangle$ where \mathcal{T} denotes the time-ordered product. We recall Wick's theorem which states that $\mathcal{T}\psi(x)\bar{\psi}(y)$ reduces to the normal product $:\psi(x)\bar{\psi}(y):$ plus the contraction of the two field operators. When considering the perturbative quark propagator, $S_F^{(0)}(x, y)$, the time-ordered product is taken with respect to a trivial vacuum for which the expectation value of $:\bar{\psi}\psi:$ vanishes. Long-range, non-perturbative physics is then at the origin of a non-vanishing $\langle : \bar{\psi}\psi : \rangle$.

(In order to establish the connection between spontaneous chiral symmetry breaking and the non-vanishing chiral condensate in a more formal way, introduce the pseudoscalar operator $P_a(x) = \bar{\psi}(x)\gamma_5\tau_a\psi(x)$ and derive the (equal-time) commutator relation $[Q_a^A, P_b] = -\delta_{ab}\bar{\psi}\psi$ which involves the axial charge Q_a^A of eq.(5). Taking the ground state expectation value, we see that $Q_a^A|0\rangle \neq 0$ is indeed consistent with $\langle \bar{\psi}\psi \rangle \neq 0$.)

Let $|\pi_a(p)\rangle$ be the state vectors of the Goldstone bosons associated with the spontaneous breakdown of chiral symmetry. Their four-momenta are denoted $p^\mu = (E_p, \mathbf{p})$, and we choose the standard normalization

$$\langle \pi_a(p) | \pi_b(p') \rangle = 2E_p \delta_{ab} (2\pi)^3 \delta^3(\mathbf{p} - \mathbf{p}'). \quad (8)$$

Goldstone's theorem also implies non-vanishing matrix elements of the axial current (4) which connect $|\pi_a(p)\rangle$ with the vacuum:

$$\langle 0 | A_a^\mu(x) | \pi_b(p) \rangle = i p^\mu f \delta_{ab} e^{-i p \cdot x}, \quad (9)$$

where f is the pion decay constant (taken here in the chiral limit, i. e. for vanishing quark mass). Its physical value

$$f_\pi = (92.4 \pm 0.3) \text{ MeV} \quad (10)$$

differs from f by a small correction linear in the quark mass m_q .

Non-zero quark masses $m_{u,d}$ shift the mass of the Goldstone boson from zero to the observed value of the physical pion mass, m_π . The connection between m_π and the u - and d - quark masses is provided by PCAC and the Gell-Mann, Oakes, Renner (GOR) relation [16]:

$$m_\pi^2 = -\frac{1}{f^2} (m_u + m_d) \langle \bar{q}q \rangle + \mathcal{O}(m_{u,d}^2). \quad (11)$$

We have set $\langle \bar{q}q \rangle \equiv \langle \bar{u}u \rangle \simeq \langle \bar{d}d \rangle$ making use of isospin symmetry which is valid to a good approximation. Neglecting terms of order $m_{u,d}^2$, identifying $f = f_\pi = 92.4$ MeV to this order and inserting $m_u + m_d \simeq 12$ MeV [17, 18] (at a renormalisation scale of order 1 GeV), one obtains

$$\langle \bar{q}q \rangle \simeq -(240 \text{ MeV})^3 \simeq -1.8 \text{ fm}^{-3}. \quad (12)$$

This condensate (or correspondingly, the pion decay constant f_π) is a measure of spontaneous chiral symmetry breaking. The non-zero pion mass, on the other hand, reflects the explicit symmetry breaking by the small quark masses, with $m_\pi^2 \sim m_q$. It is important to note that m_q and $\langle \bar{q}q \rangle$ are both scale dependent quantities. Only their product $m_q \langle \bar{q}q \rangle$ is invariant under the renormalization group.

In order to appreciate the strength of the scalar condensate (12) from a nuclear physics point of view, note that its magnitude is more than a factor of ten larger than the baryon density in the bulk of a heavy nucleus, $\rho \simeq 0.16 \text{ fm}^{-3}$.

2.4 The nucleon mass and the gap in the hadron spectrum

In the hadronic phase of QCD in which nuclei reside, confinement implies that the active ("effective") degrees of freedom are not elementary quarks and gluons but mesons and baryons. The observed spectrum of low-mass hadrons has a characteristic gap, $\Delta \sim M_N \sim 1$ GeV, which separates the masses of all baryons and almost all mesons from the ground state $|0\rangle$. On the other hand, the lightest pseudoscalar mesons are positioned well within this gap, for good reason: as Goldstone bosons of spontaneously broken chiral symmetry, pions would start out massless. Explicit

symmetry breaking by the masses m_q of the light quarks introduces perturbations on a scale small compared to Δ .

The appearance of the gap Δ is thought to be closely linked to the presence of the chiral condensate $\langle\bar{\psi}\psi\rangle$ in the QCD ground state. For example, Ioffe's formula [19], based on QCD sum rules, connects the nucleon mass M_N directly with $\langle\bar{\psi}\psi\rangle$ in leading order:

$$M_N = -\frac{4\pi^2}{\Lambda_B^2}\langle\bar{\psi}\psi\rangle + \dots \quad , \quad (13)$$

where $\Lambda_B \sim 1$ GeV is an auxiliary scale (the Borel mass) which separates "short" and "long"-distance physics in the QCD sum rule analysis. While this formula is not very accurate and needs to be improved by including higher order condensates, it nevertheless demonstrates that spontaneous chiral symmetry breaking plays an essential role in giving the nucleon its mass.

The condensate $\langle\bar{\psi}\psi\rangle$ is encoded in the pion decay constant f_π through the GOR relation (11). In the chiral limit ($m_q \rightarrow 0$), this f_π is the only quantity which can serve to define a mass scale ("transmuted" through non-perturbative dynamics from the scale $\Lambda_{QCD} \simeq 0.2$ GeV appearing in the QCD running coupling strength). It is common to introduce $4\pi f_\pi \sim 1$ GeV as the scale characteristic of spontaneous chiral symmetry breaking. This scale is then roughly identified with the spectral gap Δ .

At a more basic level, the nucleon mass is determined by the energy-momentum tensor $T^{\mu\nu}$ derived from the QCD Lagrangian (1). The component $T^{00} = H$ defines the Hamiltonian, and $M_N = \langle N|H|N\rangle$. A detailed analysis [20] shows that roughly 2/3 of M_N can be thought of as having its origin in the gluon field energy; the remainder results from the combination of quark kinetic and potential energies. Alternatively, one can express the nucleon mass as the expectation value $M_N = \langle N|T_\mu^\mu|N\rangle$ of the non-vanishing trace

$$T_\mu^\mu = \frac{\beta(g)}{2g}G_{\mu\nu}G^{\mu\nu} + m_u\bar{u}u + m_d\bar{d}d + \dots \quad , \quad (14)$$

of the energy-momentum tensor (the so-called trace anomaly - see e.g. ref.[21]). Here $G^{\mu\nu}$ is the gluonic field strength tensor and $\beta(g)$ is the beta function of QCD ($\beta = -\beta_0 g^3/(4\pi)^2$ in leading order, with $\beta_0 = 11 - 2N_f/3$). The quark mass terms³ $m_q\bar{q}q$ with $q = u, d \dots$ include light as well as heavier quarks. The physical nucleon mass M_N is expressed as

$$M_N = M_0 + \sigma_N \quad (15)$$

in terms of its evidently non-vanishing value in the chiral limit,

$$M_0 = \langle N|\frac{\beta}{2g}G_{\mu\nu}G^{\mu\nu} + \dots|N\rangle \quad (16)$$

(where the dots refer to possible contributions from heavier quarks, other than u and d), and the sigma term

$$\sigma_N = \sum_{q=u,d} m_q \frac{dM_N}{dm_q} = \langle N|m_u\bar{u}u + m_d\bar{d}d|N\rangle. \quad (17)$$

³ We have omitted here the anomalous dimension of the mass operator, as in [20].

This sigma term represents the contribution from explicit chiral symmetry breaking to the nucleon mass, through the small but non-vanishing u - and d -quark masses.

Relations such as Eq.(13), when combined with Eq.(16), give important hints. Non-perturbative gluon dynamics confines quarks and generates hadron masses, producing a gap in the spectrum. In the sector of the (almost) massless u - and d - quarks, this gap reflects the spontaneously broken chiral symmetry. Systems characterized by an energy gap usually exhibit qualitative changes when exposed to variations of thermodynamic conditions. A typical example is the temperature dependence of the gap in a superconductor. For the physics in the hadronic phase of QCD, the following key issues need therefore to be addressed: how does the quark condensate $\langle\bar{\psi}\psi\rangle$ change with temperature and/or baryon density? Are there systematic changes of hadronic spectral functions in a dense and hot medium, which would indicate changes of the QCD vacuum structure? How does the nucleon mass itself vary under such conditions? And what is the impact of these considerations on nuclear many-body systems? The sigma term (17) will play an important role in this discussion as it controls the leading density dependence of the chiral condensate (see Section 2.7).

2.5 Chiral effective field theory

The mass scale given by the gap $\Delta \sim 4\pi f_\pi$ offers a natural separation between "light" and "heavy" (or, correspondingly, "fast" and "slow") degrees of freedom. The basic idea of an effective field theory is to introduce the active light particles as collective degrees of freedom, while the heavy particles are frozen and treated as (almost) static sources. The dynamics is described by an effective Lagrangian which incorporates all relevant symmetries of the underlying fundamental theory. We now list the necessary steps, first for the pure meson sector (baryon number $B = 0$) and later for the $B = 1$ sector. We work mostly with two quark flavours ($N_f = 2$) in the following.

a) The elementary quarks and gluons of QCD are replaced by Goldstone bosons. They are represented by a 2×2 matrix field $U(x) \in SU(2)$ which collects the three isospin components $\pi_a(x)$ of the Goldstone pion. A convenient choice of coordinates is

$$U(x) = \exp[i\tau_a\phi_a(x)] \quad , \quad (18)$$

with $\phi_a = \pi_a/f$ where the pion decay constant f in the chiral limit provides a suitable normalisation. (Other choices, such as $U = \sqrt{1 - \pi_a^2/f^2} + i\tau_a\pi_a/f$, are also common. Results obtained from the effective theory must be independent of the coordinates used.)

b) Goldstone bosons interact weakly at low energy. In fact, if $|\pi\rangle = Q^A|0\rangle$ is a massless state with $H|\pi\rangle = 0$, then a state $|\pi^n\rangle = (Q^A)^n|0\rangle$ with n Goldstone bosons is also massless since the axial charges Q^A all commute with the full Hamiltonian H . Interactions between Goldstone bosons must therefore vanish at zero momentum and in the chiral limit.

c) The QCD Lagrangian (1) is replaced by an effective Lagrangian which involves the field $U(x)$ and its derivatives:

$$\mathcal{L}_{QCD} \rightarrow \mathcal{L}_{eff}(U, \partial U, \partial^2 U, \dots). \quad (19)$$

Goldstone bosons do not interact unless they carry non-zero four-momentum, so the low-energy expansion of (19) is an ordering in powers of $\partial_\mu U$. Lorentz invariance permits only even numbers of derivatives. We write

$$\mathcal{L}_{eff} = \mathcal{L}_\pi^{(2)} + \mathcal{L}_\pi^{(4)} + \dots \quad (20)$$

and omit an irrelevant constant term. The leading term, called non-linear sigma model, involves two derivatives:

$$\mathcal{L}_\pi^{(2)} = \frac{f^2}{4} \text{Tr}[\partial_\mu U^\dagger \partial^\mu U]. \quad (21)$$

At fourth order, the terms permitted by symmetries are (apart from an extra contribution from the QCD anomaly, not included here):

$$\mathcal{L}_\pi^{(4)} = \frac{l_1}{4} (\text{Tr}[\partial_\mu U^\dagger \partial^\mu U])^2 + \frac{l_2}{4} \text{Tr}[\partial_\mu U^\dagger \partial_\nu U] \text{Tr}[\partial^\mu U^\dagger \partial^\nu U], \quad (22)$$

and so forth. The constants l_1, l_2 (following canonical notations of ref. [22]) must be determined by experiment. To the extent that the effective Lagrangian includes all terms dictated by the symmetries, the effective theory is equivalent to QCD [23].

d) The symmetry breaking mass term is small, so that it can be handled perturbatively, together with the power series in momentum. The leading contribution introduces a term linear in the quark mass matrix m :

$$\mathcal{L}_\pi^{(2)} = \frac{f^2}{4} \text{Tr}[\partial_\mu U^\dagger \partial^\mu U] + \frac{f^2}{2} B_0 \text{Tr}[m(U + U^\dagger)]. \quad (23)$$

The fourth order term $\mathcal{L}_\pi^{(4)}$ also receives symmetry breaking contributions with additional constants l_i .

When expanding $\mathcal{L}^{(2)}$ to terms quadratic in the pion field, one finds

$$\mathcal{L}_\pi^{(2)} = (m_u + m_d) f^2 B_0 + \frac{1}{2} \partial_\mu \pi_a \partial^\mu \pi_a - \frac{1}{2} (m_u + m_d) B_0 \pi_a^2 + 0(\pi^4). \quad (24)$$

At this point we can immediately verify the GOR relation (11) at the level of the effective theory. The first (constant) term in (24) corresponds to the shift of the vacuum energy density by the non-zero quark masses. Identifying this with the vacuum expectation value of the corresponding piece in the QCD Lagrangian (1), we find $-(m_u \langle \bar{u}u \rangle + m_d \langle \bar{d}d \rangle) = (m_u + m_d) f^2 B_0$ and therefore $\langle \bar{u}u \rangle = \langle \bar{d}d \rangle = -f^2 B_0$ in the chiral limit, $m_{u,d} \rightarrow 0$. The pion mass term in (24) is evidently identified as $m_\pi^2 = (m_u + m_d) B_0$. Inserting B_0 , we have the GOR relation.

e) Given the effective Lagrangian, the framework for systematic perturbative calculations of the S-matrix involving Goldstone bosons, named Chiral Perturbation Theory (ChPT), is then defined by the following rules:

Collect all Feynman diagrams generated by \mathcal{L}_{eff} . Classify all terms according to powers of a variable Q which stands generically for three-momentum or energy of the Goldstone bosons, or for the pion mass m_π . The small expansion parameter is $Q/4\pi f_\pi$. Loops are subject to dimensional regularization and renormalization.

2.6 Effective Lagrangian including baryons

The prominent role played by the pion as a Goldstone boson of spontaneously broken chiral symmetry has its strong impact on the low-energy structure and dynamics of nucleons as well. Decades of research in nuclear physics have established the pion as the mediator of the long-range force between nucleons. When probing the individual nucleon itself with long-wavelength electroweak fields, a substantial part of the response comes from the pion cloud, the “soft” surface of the nucleon.

The calculational framework for this, baryon chiral perturbation theory, has been applied quite successfully to a variety of low-energy processes (such as threshold pion photo- and electroproduction and Compton scattering on the nucleon) for which increasingly accurate experimental data have become available in recent years. An introductory survey is given in chapter 7 of ref. [15]. A detailed review can be found in ref. [24].

Let us consider the sector with baryon number $B = 1$ and concentrate on the physics of the pion-nucleon system, restricting ourselves to the case of $N_f = 2$ flavours.

The nucleon is represented by a Dirac spinor field $\Psi_N(x) = (p, n)^T$ organised as an isospin-1/2 doublet of proton and neutron. The free field Lagrangian

$$\mathcal{L}_0^N = \bar{\Psi}_N(i\gamma_\mu\partial^\mu - M_0)\Psi_N \quad (25)$$

includes the nucleon mass in the chiral limit, M_0 . Note that nucleons, unlike pions, supposedly have at least part of their large mass connected with the strong scalar mean field provided by the quark condensate $\langle\bar{\psi}\psi\rangle$. Such a relationship is explicit, for example, in the Ioffe formula (13).

We can now construct the low-energy effective Lagrangian for pions interacting with a nucleon. The previous pure meson Lagrangian is replaced by $\mathcal{L}_{eff} = \mathcal{L}_\pi^{(2)} + \mathcal{L}_\pi^{(4)} + \dots + \mathcal{L}_{eff}^N$ which also includes the nucleon field. The additional term involving the nucleon is expanded again in powers of derivatives (external momenta) and quark masses:

$$\mathcal{L}_{eff}^N = \mathcal{L}_{\pi N}^{(1)} + \mathcal{L}_{\pi N}^{(2)} \dots \quad (26)$$

Let us discuss the leading term, $\mathcal{L}_{\pi N}^{(1)}$. The modifications as compared to the free nucleon Lagrangian (25) are twofold. First, there is a replacement of the ∂^μ term by a chiral covariant derivative which introduces vector current couplings between the pions and the nucleon. Secondly, there is an axial vector coupling. This structure of the πN effective Lagrangian is again dictated by chiral symmetry. We have

$$\mathcal{L}_{\pi N}^{(1)} = \bar{\Psi}_N[i\gamma_\mu(\partial^\mu - iv^\mu) + \gamma_\mu\gamma_5 a^\mu - M_0]\Psi_N \quad , \quad (27)$$

with vector and axial vector quantities involving the Goldstone boson (pion) fields in the form $\xi = \sqrt{U}$:

$$v^\mu = \frac{i}{2}(\xi^\dagger\partial^\mu\xi + \xi\partial^\mu\xi^\dagger) = -\frac{1}{4f^2}\varepsilon_{abc}\tau_a\pi_b\partial^\mu\pi_c + \dots \quad , \quad (28)$$

$$a^\mu = \frac{i}{2}(\xi^\dagger\partial^\mu\xi - \xi\partial^\mu\xi^\dagger) = -\frac{1}{2f^2}\tau_a\partial^\mu\pi_a + \dots \quad , \quad (29)$$

where the last steps result when expanding v^μ and a^μ to leading order in the pion fields.

So far, the only parameters that enter are the nucleon mass, M_0 , and the pion decay constant, f , both taken in the chiral limit and ultimately connected with a single scale characteristic of non-perturbative QCD and spontaneous chiral symmetry breaking.

When adding electroweak interactions to this scheme, one observes an additional feature which has its microscopic origin in the substructure of the nucleon, not resolved at the level of the low-energy effective theory. The analysis of neutron beta decay ($n \rightarrow pe\bar{\nu}$) reveals that the $\gamma_\mu\gamma_5$ term in (27) is to be multiplied by the axial vector coupling constant g_A , with the empirical value

$$g_A = 1.267 \pm 0.003 \quad . \quad (30)$$

At next-to-leading order ($\mathcal{L}_{\pi N}^{(2)}$), the symmetry breaking quark mass term enters. It has the effect of shifting the nucleon mass from its value in the chiral limit to the physical one, introducing the sigma term σ_N of Eq.(17). The empirical sigma term,

$$\sigma_N = (45 \pm 8) \text{MeV} \quad , \quad (31)$$

has been deduced by a sophisticated extrapolation of low-energy pion-nucleon data using dispersion relation techniques [25]. There is still an ongoing debate, related to different ways of handling the πN phase shift analysis, whether σ_N could in fact be larger than that given in (31). On the other hand, a recent extrapolation of two-flavour lattice QCD results using methods of chiral effective field theory [26] yields⁴ $\sigma_N = (47 \pm 3) \text{MeV}$, perfectly consistent with Eq.(31).

Up to this point, the πN effective Lagrangian, expanded to second order in the pion field, has the form

$$\begin{aligned} \mathcal{L}_{eff}^N = & \bar{\Psi}_N (i\gamma_\mu \partial^\mu - M_N) \Psi_N - \frac{g_A}{2f_\pi} \bar{\Psi}_N \gamma_\mu \gamma_5 \boldsymbol{\tau} \Psi_N \cdot \partial^\mu \boldsymbol{\pi} \\ & - \frac{1}{4f_\pi^2} \bar{\Psi}_N \gamma_\mu \boldsymbol{\tau} \Psi_N \cdot \boldsymbol{\pi} \times \partial^\mu \boldsymbol{\pi} + \frac{\sigma_N}{f_\pi^2} \bar{\Psi}_N \Psi_N \boldsymbol{\pi}^2 + \dots \quad , \end{aligned} \quad (32)$$

where we have not shown a series of additional terms of order $(\partial^\mu \boldsymbol{\pi})^2$ included in the complete $\mathcal{L}_{\pi N}^{(2)}$. These terms come with further constants that need to be fitted to experimental data. In later applications using in-medium chiral perturbation theory, the calculations will be based on the leading terms, linear in the derivative $\partial^\mu \boldsymbol{\pi}$ of the pion field, while the term involving σ_N will be manifest in the density dependence of the chiral condensate, as we shall see now.

2.7 Chiral thermodynamics

Before turning our attention to the nuclear many-body system, it is of some relevance to examine the thermodynamics based on the chiral effective Lagrangian $\mathcal{L}_{eff} = \sum_i (\mathcal{L}_\pi^{(i)} + \mathcal{L}_{\pi N}^{(i)})$. In particular, we are interested in the question how the quark condensate $\langle \bar{q}q \rangle$ behaves with changing thermodynamic conditions.

⁴ note: statistical errors only; systematic lattice uncertainties from finite volume effects etc. still require further detailed studies.

A. Thermodynamics of the chiral condensate

Consider as a starting point the partition function

$$\mathcal{Z} = Tr \exp \left[-\frac{1}{T} \int_V d^3x (\mathcal{H} - \mu\rho) \right] , \quad (33)$$

where \mathcal{H} is the Hamiltonian density, μ denotes the chemical potential, and ρ the baryon density. The partition function at $\mu = 0$, expressed in terms of the QCD Hamiltonian H , is

$$\mathcal{Z} = Tr \exp(-H/T) = \sum_n \langle n | e^{-E_n/T} | n \rangle \quad (34)$$

with $(H - E_n)|n\rangle = 0$. Confinement implies that the eigenstates $|n\rangle$ of H are (colour-singlet) hadrons at low temperatures, below the critical $T_c \sim 0.2$ GeV for the deconfinement transition. The physics is then determined by the states of lowest mass in the spectrum $\{E_n\}$, namely the pions. At non-zero baryon chemical potential μ , nucleons enter in addition as the lowest-mass baryons. The Hamiltonian density \mathcal{H} of QCD is expressed in terms of the relevant low-energy degrees of freedom in the hadronic phase, derived from the chiral effective Lagrangian \mathcal{L}_{eff} . The quark mass term,

$$\delta\mathcal{H} = \bar{\psi}m\psi = m_u \bar{u}u + m_d \bar{d}d + \dots , \quad (35)$$

can be separated so that $\mathcal{H} = \mathcal{H}_0 + \delta\mathcal{H}$, with \mathcal{H}_0 representing the massless limit.

Now assume a homogeneous medium and consider the pressure (or the free energy density)

$$P(T, V, \mu) = -\mathcal{F}(T, V, \mu) = \frac{T}{V} \ln \mathcal{Z} . \quad (36)$$

The derivative of P with respect to a quark mass m_q of given flavour $q = u, d$ obviously produces the in-medium quark condensate, the thermal expectation value $\langle \bar{q}q \rangle_T$ as a function of temperature and chemical potentials. Subtracting vacuum quantities one finds

$$\langle \bar{q}q \rangle_{T,\rho} = \langle \bar{q}q \rangle_0 - \frac{dP(T, V, \mu)}{dm_q} , \quad (37)$$

where $\langle \bar{q}q \rangle_0$ refers to the vacuum condensate taken at $T = 0$ and $\mu = 0$. The μ -dependence of the condensate is converted into a density dependence via the relation $\rho = \partial P / \partial \mu$ at fixed T . Using the Gell-Mann, Oakes, Renner relation (11), one can rewrite Eq.(37) as

$$\frac{\langle \bar{q}q \rangle_{T,\rho}}{\langle \bar{q}q \rangle_0} = 1 + \frac{1}{f_\pi^2} \frac{dP(T, \mu)}{dm_\pi^2} . \quad (38)$$

The task is therefore to investigate how the equation of state changes, at given temperature and baryon chemical potential, when varying the quark mass (or, equivalently, the squared pion mass).

For a system of nucleons interacting with pions, the total derivative of the pressure with respect to m_π^2 reduces to

$$\frac{dP}{dm_\pi^2} = \frac{\partial P}{\partial m_\pi^2} + \frac{\partial M_N}{\partial m_\pi^2} \frac{\partial P}{\partial M_N} = \frac{\partial P}{\partial m_\pi^2} - \frac{\sigma_N}{m_\pi^2} \rho_s(T, \mu) , \quad (39)$$

with the scalar density $\rho_s = -\partial P/\partial M_N$ and the sigma term $\sigma_N = m_\pi^2 \partial M_N / \partial m_\pi^2$ translated from Eq.(17) using the GOR relation.

Next, consider the limit of low baryon density ρ at zero temperature, $T = 0$. In this case nucleons are the only relevant degrees of freedom. At sufficiently low density, i.e. when the average distance between two nucleons is much larger than the pion Compton wavelength, the nucleon mass remains at its vacuum value M_N , and one can neglect NN interactions. The pressure is that of a Fermi gas of nucleons⁵, subject only to the Pauli principle. Returning to Eqs.(38,39), we have

$$\frac{\langle \bar{q}q \rangle_\rho}{\langle \bar{q}q \rangle_0} = 1 - \frac{\sigma_N}{m_\pi^2 f_\pi^2} \rho_s \quad , \quad (40)$$

with the scalar density

$$\rho_s = -\frac{\partial P}{\partial M_N} = 4 \int_{|\mathbf{p}| \leq k_f} \frac{d^3 p}{(2\pi)^3} \frac{M_N}{\sqrt{\mathbf{p}^2 + M_N^2}} \quad , \quad (41)$$

for a system with equal number of protons and neutrons, i.e. with degeneracy factor $d = 4$ from spin and isospin. The Fermi momentum k_f is related to the baryon density by $\rho = 2k_f^3/(3\pi^2)$. At low baryon densities with $k_f^2 \ll M_N^2$, the difference between ρ_s and ρ can be neglected, so that

$$\frac{\langle \bar{q}q \rangle_\rho}{\langle \bar{q}q \rangle_0} \approx 1 - \frac{\sigma_N}{m_\pi^2 f_\pi^2} \rho \quad . \quad (42)$$

The consequences implied by this relation are quite remarkable. Using the empirical value $\sigma_N \simeq 50$ MeV of the nucleon sigma term one observes that the chiral condensate at normal nuclear matter density, $\rho = \rho_0 = 0.16 \text{ fm}^{-3}$, is expected to decrease in magnitude to less than 2/3 of its vacuum value, a significant effect that should have observable consequences already in the bulk parts of ordinary nuclei.

In the limit of low temperature and at vanishing baryon density ($\rho = 0$), pions are the only thermally active degrees of freedom in the partition function (34). This case is well described by chiral perturbation theory. The combined low-temperature and low-density behaviour is summarised as

$$\frac{\langle \bar{q}q \rangle_\rho}{\langle \bar{q}q \rangle_0} \approx 1 - \frac{T^2}{8f_\pi^2} - 0.37 \left(\frac{\sigma_N}{50 \text{ MeV}} \right) \frac{\rho}{\rho_0} + \dots \quad , \quad (43)$$

showing a rather weak leading dependence of the chiral condensate on temperature, whereas its density dependence is far more pronounced.

B. A schematic model

Consider now a schematic model for the hadronic phase of QCD, starting from an effective Lagrangian $\mathcal{L}_{eff} = \mathcal{L}_\pi + \mathcal{L}_{\pi N} + \mathcal{L}_{NN}$ in which \mathcal{L}_π is given by Eq.(24), $\mathcal{L}_{\pi N}$ is the pion-nucleon Lagrangian of Eq.(27) and additional short distance interactions between nucleons are represented by NN contact terms,

⁵ Actually, this statement needs to be modified at extremely low densities where the system turns into a gas of clusters (deuterons etc.)

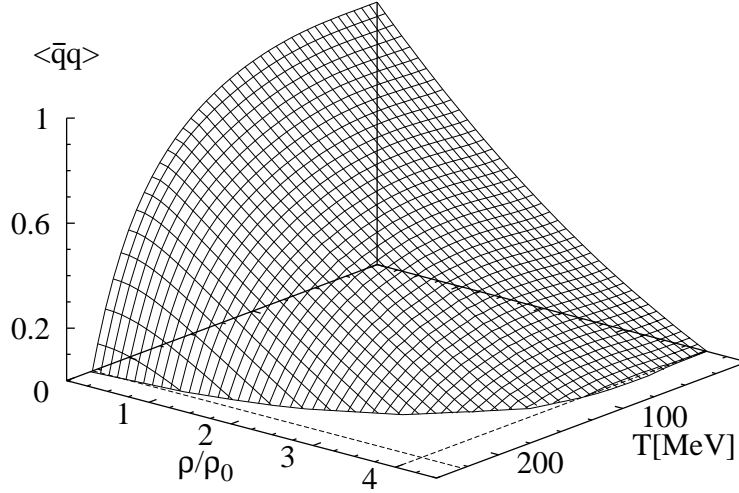


Fig. 1. Chiral condensate (in units of its vacuum value) as a function of temperature and baryon density ($\rho_0 = 0.16 \text{ fm}^{-3}$ is the density of normal nuclear matter).

$$\mathcal{L}_{NN} = -\frac{G_S}{2}(\bar{\Psi}_N\Psi_N)^2 - \frac{G_V}{2}(\bar{\Psi}_N\gamma_\mu\Psi_N)^2 + \dots \quad (44)$$

Their coupling strength parameters $G_S < 0$ and $G_V > 0$ are fixed to reproduce ground state properties of normal nuclear matter. What we have in mind here is a variant of relativistic mean field theory combined with “soft” pion fluctuations treated in the framework of chiral perturbation theory and to be discussed in more detail later.

Using two-loop thermal field theory in order to perform a self-consistent calculation of the pressure $P(T, \mu)$ in this model, one can deduce the chiral condensate as a function of temperature and baryon density following Eq.(38). This calculation generates temperature dependent mean fields for the nucleons at the same time as it treats thermal pion fluctuations with leading $\pi\pi$ interactions. The pressure equation takes the form

$$P(T, \mu) = P_N(T, \mu^*, M_N^*) + P_\pi(T, \mu^*, M_N^*) + \frac{G_S}{2}\rho_s^2 + \frac{G_V}{2}\rho^2 \quad , \quad (45)$$

with nucleon and pion contributions $P_{N,\pi}$ respectively depending on the effective nucleon mass $M_N^* = M_N + G_S \rho_s$ and the shifted baryon chemical potential $\mu^* = \mu - G_V \rho$. The baryon and scalar densities are determined as

$$\rho = \frac{\partial P}{\partial \mu} = \frac{\partial(P_N + P_\pi)}{\partial \mu^*}, \quad \rho_s = \frac{\partial P}{\partial M_N} = \frac{\partial(P_N + P_\pi)}{\partial M_N^*} \quad . \quad (46)$$

Fixing $G_{S,V}$ to the energy per particle and the equilibrium density of cold nuclear matter, one can map out the nuclear equation of state first at low temperature

and density, reproducing known physics in this domain which is a prerequisite for extrapolating into more extreme regions.

We now return to the evaluation of the chiral condensate. The dependence of $P(T, \mu)$ on the pion mass is explicit in the thermal pion Green function and implicit through the nucleon mass. The result [27] for $\langle \bar{q}q \rangle_{T, \rho}$ is shown in Fig.1. At low baryon density the linear behaviour of Eq.(42) is recovered. Pionic fluctuations, calculated up to three-loop order with inclusion of two-pion exchange effects, help maintain this approximately linear dependence not only up to $\rho \simeq \rho_0$, but even slightly beyond. Up to this point we can conclude that the magnitude of the quark condensate at normal nuclear matter density is expected to be reduced by about one third from its vacuum value, whereas the temperature dependence is far less pronounced, at least up to $T \leq 100$ MeV.

3 Chiral dynamics and the nuclear many body problem

Nuclei are aggregates of nucleons (and mesons) which are in turn clusters of quarks and gluons. Nuclei are thus central cornerstones in the QCD phase diagram. The description of nuclear many-body systems must ultimately be linked to and constrained by QCD. Recent developments using effective field theory methods are aiming to establish such connections. We focus here on a framework that relates strongly to principles of spontaneous chiral symmetry breaking in QCD and to the topics presented in the previous sections.

We propose a two-step approach. The first step emphasises the role of pions in nuclear many-body dynamics, given the rules dictated by chiral symmetry. Our strategy is based on in-medium chiral perturbation theory where the nuclear Fermi momentum enters as an additional scale in the systematic low-energy expansion of chiral effective field theory. As will be demonstrated, this approach is already capable of producing binding and saturation of nuclear matter. At the same time it gives a remarkably good value for the asymmetry energy with no additional parameter. At that level, however, important features such as the nuclear spin-orbit force cannot yet be understood. The second step is to provide strong scalar and vector mean fields, about equal in magnitude but opposite in sign, which are known phenomenologically to account for the large spin-orbit splitting in finite nuclei. These strong mean fields will be viewed as arising from the changes of the condensate structure of the QCD vacuum in the presence of the nuclear medium. QCD sum rules at finite baryon density are used for guidance to set constraints on the in-medium modifications of the relevant condensates.

3.1 Nuclear matter, part I

The present status of the nuclear matter problem can briefly be summarised as follows: a quantitatively successful description is achieved, using advanced many-body techniques [28], in a non-relativistic framework when invoking an adjustable three-body force. Complementary to such an ab-initio approach, relativistic mean field phenomenology, including non-linear terms with adjustable parameters, have also been widely used for the calculation of nuclear matter properties and finite nuclei [1].

At a more basic level, the Dirac-Brueckner method [29] solves a relativistically improved Bethe-Goldstone equation with one-boson exchange NN -interactions. The resulting Brueckner G-matrix is then used as input in Hartree-Fock calculations.

In recent years a novel approach to the NN interaction based on effective field theory (in particular, chiral perturbation theory) has emerged [30, 31, 32, 33]. Its key element is a power counting scheme which separates long- and short-distance dynamics. Methods of effective field theory have also been applied to systems of finite density [34, 35].

In the following sections the primary purpose is to point out the importance of explicit pion dynamics in the nuclear many-body problem. While pion exchange processes are well established as generators of the long and intermediate range NN interaction, their role in nuclear matter is less evident. The one-pion exchange Hartree term vanishes identically for a spin-saturated system, and the leading Fock exchange term is small. Two-pion exchange mechanisms are commonly hidden behind a purely phenomenological scalar ("sigma") field which is fitted to empirical data but has no deeper justification. This situation calls for a more detailed understanding. We report on steps in this direction, following ref. [9]. A conceptually similar strategy has been proposed in ref. [36].

Before passing on to explicit calculations it is useful to draw attention to the following fact. A simple but surprisingly good parametrization of the energy per particle, $\bar{E}(k_f) = E(k_f)/A$, of isospin symmetric nuclear matter is given in powers of the Fermi momentum k_f as

$$\bar{E}(k_f) = \frac{3k_f^2}{10 M_N} - \alpha \frac{k_f^3}{M_N^2} + \beta \frac{k_f^4}{M_N^3}, \quad (47)$$

where the nucleon density is $\rho = 2k_f^3/3\pi^2$ as usual, and M_N is the free nucleon mass. The first term is the kinetic energy of a Fermi gas. Adjusting the (dimensionless) parameters α and β to the equilibrium density, $\rho_0 = 0.16 \text{ fm}^{-3}$, ($k_{f0} = 1.33 \text{ fm}^{-1}$) and $\bar{E}_0 = \bar{E}(k_{f0}) = -16 \text{ MeV}$, gives $\alpha = 5.27$ and $\beta = 12.22$. The compression modulus $K_0 = k_{f0}^2 (\partial^2 \bar{E}(k_f) / \partial k_f^2)_{k_{f0}}$ is then predicted at $K_0 = 236 \text{ MeV}$, well in line with empirically deduced values, and the density dependence of $\bar{E}(k_f)$ using eq. (47) is remarkably close to the one resulting from the realistic many-body calculations of the Urbana group [37]. The expansion (47) in powers of Fermi momentum (rather than in powers of density) is the natural one in the context of in-medium chiral effective field theory to which we now turn our attention.

3.2 In-medium chiral perturbation theory

The tool to investigate the implications of spontaneous and explicit chiral symmetry breaking in QCD is chiral perturbation theory. Observables are calculated within the framework of an effective field theory of Goldstone bosons (pions) interacting with the lowest-mass baryons (nucleons), as described in sections 2.5 and 2.6. The diagrammatic expansion of this low-energy theory in the number of loops has a one-to-one correspondence to a systematic expansion of observables in small external momenta and the pion (or quark) mass.

In nuclear matter, the relevant momentum scale is the Fermi momentum k_f . At the empirical saturation point, $k_{f0} \simeq 2m_\pi$, so the Fermi momentum and the

pion mass are of comparable magnitude at the densities of interest. This immediately implies that pions should be included as *explicit* degrees of freedom: their propagation in matter is relevant. Pionic effects cannot be accounted for simply by adjusting coefficients of local NN contact interactions.

Both k_f and m_π are small compared to the characteristic chiral scale, $4\pi f_\pi \simeq 1.2 \text{ GeV}$. Consequently, the equation of state of nuclear matter as given by chiral perturbation theory will be represented as an expansion in powers of the Fermi momentum. The expansion coefficients are non-trivial functions of k_f/m_π , the dimensionless ratio of the two relevant scales inherent to the problem.

The chiral effective Lagrangian (27) generates the basic pion-nucleon coupling terms: the Tomozawa-Weinberg $\pi\pi NN$ contact vertex, $(1/4f_\pi^2)(q_b^\mu - q_a^\mu)\gamma_\mu\epsilon_{abc}\tau_c$, and the pseudovector πNN vertex, $(g_A/2f_\pi)q_a^\mu\gamma_\mu\gamma_5\tau_a$, where $q_{a,b}$ denote (outgoing) pion four-momenta and g_A is the axial vector coupling constant (we choose $g_A = 1.3$ so that the Goldberger-Treiman relation $g_{\pi N} = g_A M/f_\pi$ gives the empirical πN coupling constant, $g_{\pi N} = 13.2$). The only new ingredient in performing calculations at finite density (as compared to evaluations of scattering processes in vacuum) is the in-medium nucleon propagator. For a relativistic nucleon with four-momentum $p^\mu = (p_0, \mathbf{p})$ it reads

$$(\not{p} + M) \left\{ \frac{i}{p^2 - M^2 + i\varepsilon} - 2\pi\delta(p^2 - M^2)\theta(p_0)\theta(k_f - |\mathbf{p}|) \right\}. \quad (48)$$

The second term is the medium insertion which accounts for the fact that the ground state of the system has changed from an "empty" vacuum to a filled Fermi sea of nucleons. Diagrams can then be organized systematically in the number of medium insertions, and an expansion is performed in leading inverse powers of the nucleon mass, consistently with the k_f -expansion.

Our "inward-bound" strategy [9] is now as follows. One starts at large distances (small k_f) and systematically generates the pion-induced correlations between nucleons as they develop with decreasing distance (increasing k_f). The calculations of the energy density reported here are performed to 3-loop order (including terms up to order k_f^5) and incorporate one- and two-pion exchange processes. The procedure involves one single momentum space cutoff Λ which encodes dynamics at short distances not resolved explicitly in the effective low-energy theory. This high-momentum scale Λ is the only free parameter at this stage. It has to be fine-tuned. (Alternatively and equivalently, one could use dimensional regularization, remove divergent loop integrals and replace them by adjustable NN contact terms which then parametrize the unresolved short-distance physics).

Nuclear chiral dynamics up to three-loop order introduces the diagrams, Fig. 2. They include the one-pion exchange (OPE) Fock term, iterated OPE and irreducible two-pion exchange. Medium insertions are systematically applied on all nucleon propagators, and the relevant loop integrations yield results which can be written in analytic form for all pieces.

We now outline the leading contributions to the energy per particle $\bar{E}(k_f)$. The kinetic energy including first order relativistic corrections is

$$\bar{E}_{kin}(k_f) = \frac{3k_f^2}{10M_N} \left(1 - \frac{5k_f^2}{28M_N^2} \right). \quad (49)$$

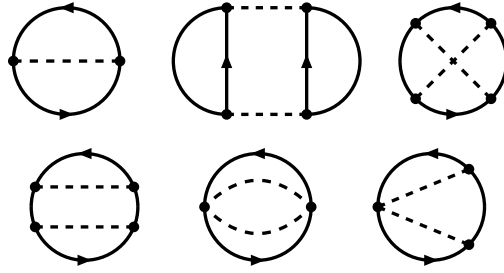


Fig. 2. In-medium chiral perturbation theory: One-pion exchange Fock term (top left), iterated one-pion exchange (top middle and right) and examples of irreducible two-pion exchange terms (bottom). See Ref. [9] for details.

Terms of order k_f^6 are already negligibly small. At least from this perspective, nuclear matter is a non-relativistic system.

The OPE Fock term (see the diagram on the left of Fig. 2) becomes

$$\bar{E}_{1\pi}(k_f) = \frac{g_A^2 m_\pi^3}{(4\pi f_\pi)^2} \left[F\left(\frac{k_f}{m_\pi}\right) + \frac{m_\pi^2}{M_N^2} G\left(\frac{k_f}{m_\pi}\right) \right], \quad (50)$$

where F and G are functions of the dimensionless variable k_f/m_π . They are given explicitly in Ref. [9]. All finite parts of iterated OPE and irreducible two-pion exchange are of the generic form

$$\bar{E}_{2\pi}(k_f) = \frac{m_\pi^4}{(4\pi f_\pi)^4} \left[g_A^4 M_N H_4\left(\frac{k_f}{m_\pi}\right) + m_\pi H_5\left(\frac{k_f}{m_\pi}\right) \right], \quad (51)$$

with the functions $H_{4,5}$ again given explicitly in Ref.[9]. All power divergences specific to cutoff regularization are summarized in the expression

$$\bar{E}_\Lambda(k_f) = \frac{\Lambda k_f^3}{(4\pi f_\pi)^4} [-10g_A^4 M_N + (3g_A^2 + 1)(g_A^2 - 1)\Lambda], \quad (52)$$

where the attractive and dominant first term in the brackets arises from iterated OPE. Note that this term, proportional to the density $\rho \sim k_f^3$, can be generated in an equivalent mean-field approach by a NN contact interaction with appropriate coupling strength. The sum of the terms (49)–(52) determines the energy per particle of nuclear matter within chiral dynamics, to the order shown in Fig. 2.

3.3 Nuclear matter equation of state

A striking feature of the chiral dynamics approach is the simplicity of the saturation mechanism for isospin-symmetric nuclear matter. Before turning to the presentation of detailed results, it is instructive first to discuss the situation in the exact chiral limit, $m_\pi = 0$. The basic saturation mechanism can already be demonstrated by truncating the one- and two-pion exchange diagrams at order k_f^4 . We can make straightforward contact with the parametrization (47) of the energy per particle

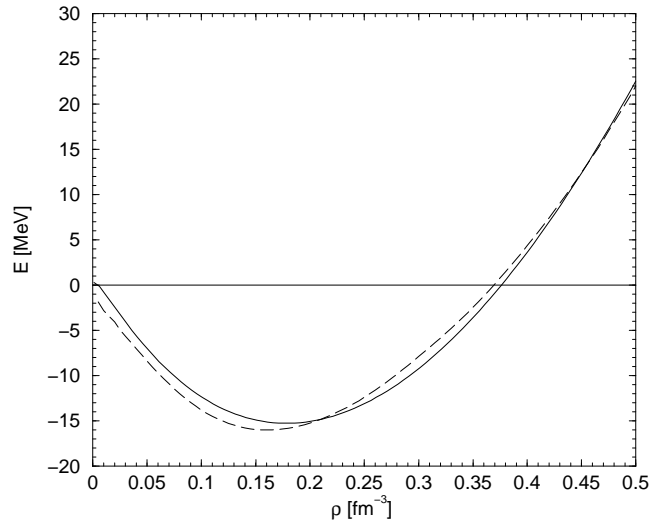


Fig. 3. Energy per particle, $\bar{E}(k_f)$, of symmetric nuclear matter derived from chiral one- and two-pion exchange (solid line) [9]. The cutoff scale is $\Lambda = 646 \text{ MeV}$. The dashed line is the result of Ref. [37].

and identify the coefficients α and β of the k_f^3 and k_f^4 terms, respectively. The result for α in the chiral limit is:

$$\alpha = \left(\frac{g_{\pi N}}{4\pi} \right)^2 \left[\frac{10\Lambda}{M_N} \left(\frac{g_{\pi N}}{4\pi} \right)^2 - 1 \right], \quad (53)$$

where we have neglected the small correction proportional to Λ^2 in Eq.(52). The strongly attractive leading term in Eq.(52) is accompanied by the (weakly repulsive) one-pion exchange Fock term. The k_f^3 -contribution to $\bar{E}(k_f)$ would lead to collapse of the many-body system. The stabilizing k_f^4 -term is controlled by the coefficient (calculated again in the chiral limit)

$$\beta = \frac{3}{70} \left(\frac{g_{\pi N}}{4\pi} \right)^4 (4\pi^2 + 237 - 24 \ln 2) - \frac{3}{56} = 13.55, \quad (54)$$

a unique and parameterfree result to this order. The two-pion exchange dynamics in combination with the Pauli exclusion principle produces repulsion of just the right magnitude to achieve saturation: the result, Eq.(54), is within 10% of the empirical $\beta = 12.2$. Adjustment of the short-distance scale Λ between 0.5 and 0.6 GeV easily leads to a stable minimum of $\bar{E}(k_f)$ in the proper range of density and binding energy.

The full 3-loop chiral dynamics result for $\bar{E}(k_f)$ in symmetric nuclear matter, using $m_\pi = 135 \text{ MeV}$ (the neutral pion mass), is shown in Fig.3 together with a realistic many-body calculation [37]. The outcome is remarkable: with one single parameter $\Lambda = 0.65 \text{ GeV}$ fixed to the value $\bar{E}_0 = -15.3 \text{ MeV}$ at equilibrium,

perturbative pion dynamics alone produces an equation of state which follows that of much more sophisticated calculations up to about three times the density of nuclear matter. The predicted compression modulus is $K_0 = 255$ MeV, well in line with the "empirical" $K_0 = (250 \pm 25)$ MeV. The basic mechanisms behind binding and saturation in this approach are thus identified as follows. The exchange of two pions between nucleons (truncated at the momentum scale Λ) drives the attraction⁶ proportional to k_f^3 in the energy per particle. The Pauli blocking of intermediate nucleon states in these 2π exchange processes produces the (repulsive) stabilizing k_f^4 term in E/A .

The calculations just described have also been extended to finite temperature [9]. The resulting pressure as function of density shows the van der Waals - like behaviour of the liquid - gas phase transition, with a critical temperature $T_c \simeq 25$ MeV, slightly larger than the value around 18 MeV commonly quoted as the "empirical" one.

3.4 Asymmetry energy

The specific isospin dependence of two-pion exchange should have its distinct influence on the behaviour of asymmetric nuclear matter, with increasing excess of neutrons over protons. We introduce as usual the asymmetry parameter $\delta = (\rho_n - \rho_p)/\rho = (N - Z)/(N + Z)$, keeping the total density $\rho = \rho_n + \rho_p = 2k_f^3/3\pi^2$ constant. The proton and neutron densities are $\rho_{p,n} = (k_f^{p,n})^3/3\pi^2$ in terms of the corresponding Fermi momenta, k_f^p and k_f^n . Without change of any input, the asymmetry energy $A(k_f)$ defined by

$$\bar{E}_{as}(k_f^p, k_f^n) = \bar{E}(k_f) + \delta^2 A(k_f) + \dots \quad (55)$$

has been calculated [9]. The result at nuclear matter density is $A_0 = A(k_{f0}) = 33.8$ MeV. This is in very good agreement with the empirical value $A_0 = (30 \pm 4)$ MeV derived from extensive fits to nuclide masses [38].

Extrapolations to higher density work roughly up to $\rho \simeq 1.5 \rho_0$. At still higher densities, there are indications that non-trivial isospin dependence at shorter distances, beyond one- and two-pion exchange, starts to play a role. A similar statement holds for pure neutron matter which comes out properly unbound, but its predicted equation of state starts to deviate from that of realistic many-body calculations at neutron densities larger than 0.2 fm^{-3} .

3.5 Nuclear mean field from chiral dynamics

The in-medium three-loop calculation of the energy per particle defines the (momentum dependent) self-energy of a single nucleon in nuclear matter up to two-loop order. The real part of the resulting single particle potential in isospin-symmetric matter at the saturation point, for a nucleon with zero momentum, comes out as [10]

$$U(p = 0, k_{f0}) = -53.2 \text{ MeV}, \quad (56)$$

⁶ In a qualitative (but not strict) analogy, these mechanisms are reminiscent of van der Waals forces.

using exactly the same one- and two-pion exchange input that has led to the solid curve in Fig. 3. The momentum dependence of $U(p, k_{f0})$ can be rephrased in terms of an average effective nucleon mass $M^* \simeq 0.8 M_N$ at nuclear matter density, and the imaginary part of the potential for a nucleon-hole at the bottom of the Fermi sea is predicted to be about 30 MeV. While these numbers are remarkably close to the empirically deduced ones, it must nevertheless be emphasised that the detailed momentum dependence of the single particle potential, as obtained in this approach, is not yet satisfactory.

3.6 Intermediate summary and a working hypothesis

Explicit pion dynamics originating from the spontaneously broken chiral symmetry of QCD is clearly an important aspect of the nuclear many-body problem. In-medium chiral perturbation theory, with one single cutoff scale $\Lambda \simeq 0.65$ GeV introduced to regularize the few divergent parts associated with two-pion exchange, gives realistic binding and saturation of nuclear matter already at three-loop order. At the same time it gives very good values for the compression modulus and the asymmetry energy. These are non-trivial observations, considering that it all works with only one adjustable parameter encoding short-distance dynamics which remains unresolved at the Fermi momenta $k_f \ll M_N \sim 4\pi f_\pi$ characteristic of equilibrium nuclear matter.

In view of the relevant scales in nuclear matter, the importance of explicit pion degrees of freedom does not come unexpected. Many of the existing models ignore pions, however. They introduce purely phenomenological scalar fields with non-linear couplings and freely adjustable parameters in order to simulate two-pion exchange effects.

Now, in order to establish contacts with the widely used and successful relativistic nuclear mean field phenomenology, the following working hypothesis suggests itself as a guide for the next necessary step. Assume that the nuclear matter ground state represents a "shifted" QCD vacuum characterized by strong vector (V) and scalar (S) condensate fields acting on the nucleons, with $V \simeq -S \simeq 0.3$ GeV as suggested e. g. by in-medium QCD sum rules [6, 7, 8]. Such a scenario would not produce binding all by itself. Binding and saturation would instead result from pionic (chiral) fluctuations as outlined previously. The strong condensate fields would, on the other hand, generate the large spin-orbit splitting in finite nuclei. This is the conceptual framework that we now apply when turning to finite nuclei.

4 Relativistic nuclear model constrained by QCD and chiral symmetry

At this point it is appropriate to recall in greater detail the relativistic nuclear phenomenology that goes under the name of Quantum Hadrodynamics (QHD) [1]: a framework of Lorentz-covariant meson-baryon effective field theories. In the mean-field approximation, such an approach is equivalent to a model with local four-point interactions between nucleons [39, 40, 41]. Models based on QHD have been successfully applied to describe a broad range of nuclear phenomena, from light nuclei to superheavy elements (see Ref. [2] for a recent review, and references therein).

This framework has also been extended to studies of the structure of exotic nuclei with extreme isospin and close to the particle drip lines.

The effective hadronic Lagrangians of QHD and related models incorporate known long-range interactions constrained by symmetries and a set of generic short-range interactions. These models are consistent with fundamental symmetries: Lorentz invariance, parity invariance, electromagnetic gauge invariance, isospin and with the chiral symmetry of QCD [1, 5, 42]. The most successful QHD models are, however, purely phenomenological, with parameters adjusted to reproduce the nuclear matter equation of state and global properties of spherical closed-shell nuclei. QHD calculations do not include pions explicitly, whereas we have just demonstrated that pions, as Goldstone bosons of spontaneously broken chiral symmetry, play an important role in the nuclear many-body problem. Two-pion exchange effects are supposedly incorporated as part of the strong scalar-isoscalar field of QHD models, but in an ad-hoc manner without detailed reference to the underlying $\pi\pi NN$ dynamics. QCD symmetries do constrain the effective QHD Lagrangians by restricting the form of possible interaction terms. However, the empirical data set of bulk and single-particle properties of finite nuclei can only determine six or seven parameters in the general expansion of the effective Lagrangian in powers of the fields and their derivatives [43]. Such a general expansion can be controlled by the “naive dimensional analysis” (NDA) [40, 41, 44, 45]. NDA tests the coefficients of the expansion for “naturalness”, i.e. this method controls the orders of magnitude of the coupling constants. NDA can exclude some interaction terms because their couplings would be “unnatural”, but it cannot determine the model parameters at the level of accuracy required for a quantitative analysis of nuclear structure data.

Our approach is similar in spirit but proceeds with a different strategy, imposing as many low-energy QCD constraints as possible in order to minimize the number of freely adjustable parameters. It is based on the conjectures already presented in the Introduction, namely:

that nuclear binding and saturation arise dominantly from chiral (pionic) fluctuations in combination with Pauli blocking effects, as described in the previous section;

that these pionic fluctuations are superimposed on individually strong scalar and vector fields of approximately equal magnitude and opposite sign, originating from density-dependent changes of the QCD vacuum condensates.

Our aim is thus to study the interplay between condensate background fields and perturbative chiral fluctuations, both rooted in the spontaneous symmetry breaking pattern of QCD, in forming nuclei. We will demonstrate how this scenario works at large. Whereas in first approximation the condensate fields do not play a significant role for the saturation mechanism, they are essential for the description of ground states of finite nuclei and, in particular, the spin-orbit force.

4.1 Point-coupling model: density dependent contact interactions

A suitable framework to address these questions, both for nuclear matter and for finite nuclei, is a relativistic point coupling model with density dependent NN contact interactions. The explicit density dependence of these couplings reflects

effects “beyond mean field” such as they arise from the Pauli corrections to two-pion exchange fluctuations discussed previously. The mapping of the k_f expansions of chiral dynamics, described in Section 3, into the form of equivalent point couplings depending on fractional powers of ρ , is performed by equating the nucleon self-energies resulting from both schemes.

A. Lagrangian

The relativistic point-coupling Lagrangian is built from basic density and current operator blocks bilinear in the Dirac spinor field Ψ of the nucleon⁷ :

$$(\bar{\Psi}\mathcal{O}_\tau\Gamma\Psi) \quad , \quad \mathcal{O}_\tau \in \{1, \tau_i\} \quad , \quad \Gamma \in \{1, \gamma_\mu, \gamma_5, \gamma_5\gamma_\mu, \sigma_{\mu\nu}\} . \quad (57)$$

Here τ_i are the isospin matrices and Γ generically denotes the Dirac matrices. The interaction terms of the Lagrangian are products of these blocks to a given order. In principle, a general effective Lagrangian can be written as a power series in the point couplings $(\bar{\Psi}\mathcal{O}_\tau\Gamma\Psi)$ and their derivatives. In practice, properties of symmetric and asymmetric nuclear matter, as well as empirical ground state properties of finite nuclei, constrain only the isoscalar-scalar, the isoscalar-vector, the isovector-vector, and to a certain extent the isovector-scalar channels.

The model that we consider here includes the following four-fermion interaction vertices:

$$\begin{aligned} \text{isoscalar-scalar:} & \quad (\bar{\Psi}\Psi)^2 \\ \text{isoscalar-vector:} & \quad (\bar{\Psi}\gamma_\mu\Psi)(\bar{\Psi}\gamma^\mu\Psi) \\ \text{isovector-scalar:} & \quad (\bar{\Psi}\boldsymbol{\tau}\Psi) \cdot (\bar{\Psi}\boldsymbol{\tau}\Psi) \\ \text{isovector-vector:} & \quad (\bar{\Psi}\boldsymbol{\tau}\gamma_\mu\Psi) \cdot (\bar{\Psi}\boldsymbol{\tau}\gamma^\mu\Psi) . \end{aligned}$$

Vectors in isospin space are denoted by boldface symbols. The model is defined by the Lagrangian density

$$\mathcal{L} = \mathcal{L}_{\text{free}} + \mathcal{L}_{4f} + \mathcal{L}_{\text{der}} + \mathcal{L}_{\text{em}}, \quad (58)$$

with the four terms specified as follows:

$$\begin{aligned} \mathcal{L}_{\text{free}} &= \bar{\Psi}(i\gamma_\mu\partial^\mu - M)\Psi , \\ \mathcal{L}_{4f} &= -\frac{1}{2} G_S(\hat{\rho})(\bar{\Psi}\Psi)(\bar{\Psi}\Psi) \\ &\quad -\frac{1}{2} G_V(\hat{\rho})(\bar{\Psi}\gamma_\mu\Psi)(\bar{\Psi}\gamma^\mu\Psi) \\ &\quad -\frac{1}{2} G_{TS}(\hat{\rho})(\bar{\Psi}\boldsymbol{\tau}\Psi) \cdot (\bar{\Psi}\boldsymbol{\tau}\Psi) \\ &\quad -\frac{1}{2} G_{TV}(\hat{\rho})(\bar{\Psi}\boldsymbol{\tau}\gamma_\mu\Psi) \cdot (\bar{\Psi}\boldsymbol{\tau}\gamma^\mu\Psi) , \\ \mathcal{L}_{\text{der}} &= -\frac{1}{2} D_S(\hat{\rho})(\partial_\nu\bar{\Psi}\Psi)(\partial^\nu\bar{\Psi}\Psi) \end{aligned} \quad (60)$$

⁷ From here on we denote the nucleon field by Ψ , dropping the index N . Similarly, the nucleon mass is denoted M without further index specification.

$$\begin{aligned}
& -\frac{1}{2} D_V(\hat{\rho})(\partial_\nu \bar{\Psi} \gamma_\mu \Psi)(\partial^\nu \bar{\Psi} \gamma^\mu \Psi) \\
& -\frac{1}{2} D_{TS}(\hat{\rho})(\partial_\nu \bar{\Psi} \tau \Psi) \cdot (\partial^\nu \bar{\Psi} \tau \Psi) \\
& -\frac{1}{2} D_{TV}(\hat{\rho})(\partial_\nu \bar{\Psi} \tau \gamma_\mu \Psi) \cdot (\partial^\nu \bar{\Psi} \tau \gamma^\mu \Psi) , \tag{61}
\end{aligned}$$

$$\mathcal{L}_{\text{em}} = +eA^\mu \bar{\Psi} \frac{1 + \tau_3}{2} \gamma_\mu \Psi - \frac{1}{4} F_{\mu\nu} F^{\mu\nu} . \tag{62}$$

While the Lagrangian (58)-(62) is going to be formally used in the mean-field approximation, fluctuations beyond mean field are nevertheless encoded in the density-dependent couplings $G_i(\hat{\rho})$ and $D_i(\hat{\rho})$, to be specified in detail later. When applied to finite nuclei the model must also include the coupling \mathcal{L}_{em} of the protons to the electromagnetic field, and the derivative terms in \mathcal{L}_{der} , in addition to the free nucleon Lagrangian $\mathcal{L}_{\text{free}}$ and the interaction terms in \mathcal{L}_{4f} . The derivative terms are built from the blocks $\partial_\nu(\bar{\Psi} \tau_i \Gamma_j \Psi)$ (the derivative is understood to act on both $\bar{\Psi}$ and Ψ). One can, of course, construct many more derivative terms of higher orders. In \mathcal{L}_{der} we include only those terms which are direct counterparts of the second order interaction terms incorporated in \mathcal{L}_{4f} . In this way we take into account leading effects of finite range interactions that are important for a quantitative fine-tuning of nuclear properties.

Our model Lagrangian formally resembles the ones used in the standard relativistic mean-field point-coupling models of Refs. [39, 40, 41, 45, 46]. The underlying dynamics is, however, quite different. The parameters of the interaction terms in the standard point-coupling models have constant values adjusted to reproduce the nuclear matter equation of state and a set of global properties of spherical closed-shell nuclei. In order to describe properties of finite nuclei on a quantitative level, these models include also some higher order interaction terms, such as six-fermion vertices $(\bar{\Psi} \Psi)^3$, and eight-fermion vertices $(\bar{\Psi} \Psi)^4$ and $[(\bar{\Psi} \gamma_\mu \Psi)(\bar{\Psi} \gamma^\mu \Psi)]^2$. Our approach includes only second order interaction terms, but with coupling strengths that are functions of the nucleon density operator $\hat{\rho}$. Their functional dependence will be determined by matching the nucleon self-energies resulting from in-medium chiral perturbation theory and finite-density QCD sum rules.

Medium dependent vertex functions have also been considered in so-called density dependent relativistic hadron field (DDRH) models. The density dependent meson-nucleon vertex functions are determined either by mapping the nuclear matter Dirac-Brueckner nucleon self-energies in the local density approximation [47, 48, 49], or they are adjusted to reproduce properties of symmetric and asymmetric nuclear matter and finite nuclei [50, 51]. In practical applications of the DDRH models the meson-nucleon couplings are assumed to be functions of the baryon density $\Psi^\dagger \Psi$. In a relativistic framework the couplings can also depend on the scalar density $\bar{\Psi} \Psi$. Nevertheless, expanding in $\Psi^\dagger \Psi$ is the natural choice, for several reasons. The baryon density is connected to the conserved baryon number, unlike the scalar density for which no conservation law exists. The scalar density is a dynamical quantity, to be determined self-consistently by the equations of motion, and expandable in powers of the Fermi momentum. For the meson exchange models it has been shown that the dependence on baryon density alone provides a more direct relation between the self-energies of the density-dependent hadron field theory and the Dirac-Brueckner microscopic self-energies [49]. Moreover, the pion-exchange contributions to the nucleon self-energy, as calculated using in-medium

chiral perturbation theory, are directly given as expansions in powers of the Fermi momentum. Following these considerations, we express the coupling strengths of the interaction terms as functions of the baryon density, represented by the operator $\hat{\rho} = \Psi^\dagger \Psi$ in the rest frame of the many-body system.

B. Equation of motion and nucleon self-energies

The single-nucleon Dirac equation is derived by variation of the Lagrangian (58) with respect to $\bar{\Psi}$:

$$[\gamma_\mu(i\partial^\mu - V^\mu) - (M + S)]\Psi = 0, \quad (63)$$

where

$$V^\mu = \Sigma^\mu + \boldsymbol{\tau} \cdot \boldsymbol{\Sigma}_T^\mu + \Sigma_r^\mu + \boldsymbol{\tau} \cdot \boldsymbol{\Sigma}_{rT}^\mu \quad (64)$$

and

$$S = \Sigma_S + \boldsymbol{\tau} \cdot \boldsymbol{\Sigma}_{TS} + \Sigma_{rS} + \boldsymbol{\tau} \cdot \boldsymbol{\Sigma}_{rTS}, \quad (65)$$

with the nucleon self-energies defined by the following relations

$$\Sigma^\mu = (G_V - D_V \square) j^\mu - e A^\mu \frac{1 + \tau_3}{2} \quad (66)$$

$$\boldsymbol{\Sigma}_T^\mu = (G_{TV} - D_{TV} \square) \mathbf{j}_T^\mu \quad (67)$$

$$\Sigma_S = (G_S - D_S \square) (\bar{\Psi} \Psi) \quad (68)$$

$$\boldsymbol{\Sigma}_{TS} = (G_{TS} - D_{TS} \square) (\bar{\Psi} \boldsymbol{\tau} \Psi) \quad (69)$$

$$\Sigma_{rS} = -\frac{\partial D_S}{\partial \hat{\rho}} (\partial_\nu j^\mu) u_\mu (\partial^\nu (\bar{\Psi} \Psi)) \quad (70)$$

$$\boldsymbol{\Sigma}_{rTS} = -\frac{\partial D_{TS}}{\partial \hat{\rho}} (\partial_\nu j^\mu) u_\mu (\partial^\nu (\bar{\Psi} \boldsymbol{\tau} \Psi)) \quad (71)$$

$$\boldsymbol{\Sigma}_{rT}^\mu = -\frac{\partial D_{TV}}{\partial \hat{\rho}} (\partial_\nu j^\alpha) u_\alpha (\partial^\nu \mathbf{j}_T^\mu) \quad (72)$$

$$\begin{aligned} \Sigma_r^\mu = u^\mu & \left(\frac{1}{2} \frac{\partial G_S}{\partial \hat{\rho}} (\bar{\Psi} \Psi) (\bar{\Psi} \Psi) + \frac{1}{2} \frac{\partial D_S}{\partial \hat{\rho}} (\partial^\nu (\bar{\Psi} \Psi)) (\partial_\nu (\bar{\Psi} \Psi)) \right. \\ & + \frac{1}{2} \frac{\partial G_{TS}}{\partial \hat{\rho}} (\bar{\Psi} \boldsymbol{\tau} \Psi) \cdot (\bar{\Psi} \boldsymbol{\tau} \Psi) + \frac{1}{2} \frac{\partial D_{TS}}{\partial \hat{\rho}} (\partial^\nu (\bar{\Psi} \boldsymbol{\tau} \Psi)) \cdot (\partial_\nu (\bar{\Psi} \boldsymbol{\tau} \Psi)) \\ & + \frac{1}{2} \frac{\partial G_V}{\partial \hat{\rho}} j^\nu j_\nu + \frac{1}{2} \frac{\partial D_V}{\partial \hat{\rho}} (\partial_\nu j_\alpha) (\partial^\nu j^\alpha) \\ & + \frac{1}{2} \frac{\partial G_{TV}}{\partial \hat{\rho}} \mathbf{j}_T^\nu \cdot \mathbf{j}_{T\nu} + \frac{1}{2} \frac{\partial D_{TV}}{\partial \hat{\rho}} (\partial_\nu \mathbf{j}_{T\alpha}) \cdot (\partial^\nu \mathbf{j}_T^\alpha) \left. \right) \\ & - \frac{\partial D_V}{\partial \hat{\rho}} (\partial_\nu j_\alpha) u^\alpha (\partial^\nu j^\mu). \end{aligned} \quad (73)$$

The nucleon isoscalar and isovector currents read

$$j^\mu = \bar{\Psi} \gamma^\mu \Psi, \quad (74)$$

$$\mathbf{j}_T^\mu = \bar{\Psi} \boldsymbol{\tau} \gamma^\mu \Psi, \quad (75)$$

respectively. We write $\hat{\rho} u^\mu = j^\mu$ and the four-velocity u^μ is defined as $(1 - \mathbf{v}^2)^{-1/2} (1, \mathbf{v})$ where \mathbf{v} is the three-velocity vector ($\mathbf{v} = 0$ in the rest-frame of the nuclear system). In addition to the isoscalar-vector Σ^μ , isoscalar-scalar Σ_S ,

isovector-vector Σ_T^μ and isovector-scalar Σ_{TS} self-energies, the density dependence of the vertex functions produces the *rearrangement* contributions Σ_{rS} , Σ_r^μ , Σ_{rTS} and Σ_{rT}^μ . The rearrangement terms result from the variation of the vertex functionals with respect to the baryon fields in the density operator $\hat{\rho}$ (which coincides with the baryon density in the nuclear matter rest-frame). For a model with density dependent couplings, the inclusion of the rearrangement self-energies is essential for energy-momentum conservation $\partial_\mu T^{\mu\nu} = 0$, and thermodynamical consistency $\rho^2 \frac{\partial}{\partial \rho} \left(\frac{\varepsilon}{\rho} \right) = \frac{1}{3} \sum_{i=1}^3 T^{ii}$ (i.e. for the pressure equation derived from the thermodynamic definition and from the energy-momentum tensor) [47, 50].

When applied to nuclear matter or ground-state properties of finite nuclei, the point-coupling model is understood to be used in the mean-field approximation. The ground state of a nucleus with A nucleons is the product of the lowest occupied single-nucleon self-consistent stationary solutions of the Dirac equation (63). The ground state energy is the sum of the single-nucleon energies plus a functional of the scalar density,

$$\rho_s = \sum_{k=1}^A \bar{\psi}_k \psi_k, \quad (76)$$

and of the baryon density of the nucleons,

$$\rho = \sum_{k=1}^A \psi_k^\dagger \psi_k, \quad (77)$$

where the sums run over occupied positive-energy single-nucleon states $|k\rangle$ with wave functions ψ_k .

The density dependence of the coupling strengths which determine the self-energies (66-73), will be constrained by in-medium QCD sum rules and chiral pion dynamics, to be specified in detail in the following sections

4.2 Nuclear matter, part II

In translationally invariant infinite nuclear matter all terms involving the derivative couplings (61) drop out and the single-nucleon Dirac equation reads

$$[\gamma_\mu (i\partial^\mu - \Sigma^\mu - \Sigma_r^\mu - \boldsymbol{\tau} \cdot \boldsymbol{\Sigma}_T^\mu) - (M + \Sigma_S + \boldsymbol{\tau} \cdot \boldsymbol{\Sigma}_{TS})]\Psi = 0, \quad (78)$$

where the self-energies are

$$\Sigma^\mu = G_V j^\mu, \quad (79)$$

$$\Sigma_r^\mu = u^\mu \left[\frac{1}{2} \frac{\partial G_S}{\partial \hat{\rho}} (\bar{\Psi}\Psi)(\bar{\Psi}\Psi) + \frac{1}{2} \frac{\partial G_V}{\partial \hat{\rho}} j^\nu j_\nu + \frac{1}{2} \frac{\partial G_{TS}}{\partial \hat{\rho}} (\bar{\Psi}\boldsymbol{\tau}\Psi) \cdot (\bar{\Psi}\boldsymbol{\tau}\Psi) + \frac{1}{2} \frac{\partial G_{TV}}{\partial \hat{\rho}} \mathbf{j}_T^\nu \cdot \mathbf{j}_{T\nu} \right], \quad (80)$$

$$\Sigma_T^\mu = G_{TV} \mathbf{j}_T^\mu, \quad (81)$$

$$\Sigma_S = G_S (\bar{\Psi}\Psi), \quad (82)$$

$$\Sigma_{TS} = G_{TS} (\bar{\Psi}\boldsymbol{\tau}\Psi). \quad (83)$$

The total isoscalar vector self-energy includes the rearrangement contributions Σ_r^μ . In nuclear matter at rest the spatial components of the four-currents vanish, and the densities are calculated by taking expectation values

$$\rho_s = \langle \Phi | \bar{\Psi} \Psi | \Phi \rangle, \quad (84)$$

$$\rho = \langle \Phi | \bar{\Psi} \gamma^0 \Psi | \Phi \rangle, \quad (85)$$

$$\rho_{s3} = \langle \Phi | \bar{\Psi} \tau_3 \Psi | \Phi \rangle, \quad (86)$$

$$\rho_3 = \langle \Phi | \bar{\Psi} \tau_3 \gamma^0 \Psi | \Phi \rangle, \quad (87)$$

where $|\Phi\rangle$ is the nuclear matter ground state. The energy density \mathcal{E} and the pressure P are derived from the energy-momentum tensor $T^{\mu\nu}$ as

$$\mathcal{E} = \mathcal{E}_{kin}^n + \mathcal{E}_{kin}^p - \frac{1}{2} G_S \rho_s^2 - \frac{1}{2} G_{TS} \rho_{s3}^2 + \frac{1}{2} G_V \rho^2 + \frac{1}{2} G_{TV} \rho_3^2, \quad (88)$$

$$\begin{aligned} P = & \tilde{E}_p \rho_p + \tilde{E}_n \rho_n - \mathcal{E}_{kin}^p - \mathcal{E}_{kin}^n + \frac{1}{2} G_V \rho^2 + \frac{1}{2} G_{TV} \rho_3^2 + \frac{1}{2} G_S \rho_s^2 + \frac{1}{2} G_{TS} \rho_{s3}^2 \\ & + \frac{1}{2} \frac{\partial G_S}{\partial \rho} \rho_s^2 \rho + \frac{1}{2} \frac{\partial G_V}{\partial \rho} \rho^3 + \frac{1}{2} \frac{\partial G_{TV}}{\partial \rho} \rho_3^2 \rho + \frac{1}{2} \frac{\partial G_{TS}}{\partial \rho} \rho_{s3}^2 \rho. \end{aligned} \quad (89)$$

The baryon density is related to the Fermi momentum k_f in the usual way,

$$\rho_i = \frac{2}{(2\pi)^3} \int_{|k| \leq k_f^i} d^3 k = \frac{(k_f^i)^3}{3\pi^2}, \quad (90)$$

where the index $i = \{p, n\}$ refers to protons and neutrons, respectively. The corresponding scalar densities are determined by the self-consistency relation

$$\rho_s^i = \frac{2}{(2\pi)^3} \int_{|k| \leq k_f^i} d^3 k \frac{M_i^*}{\sqrt{k^2 + (M_i^*)^2}} = \frac{M_i^*}{2\pi^2} \left[k_f^i \tilde{E}_i - (M_i^*)^2 \ln \frac{k_f^i + \tilde{E}_i}{M_i^*} \right], \quad (91)$$

with the proton and neutron quasi-particle energies

$$\tilde{E}_i = \sqrt{(k_f^i)^2 + (M_i^*)^2}, \quad (92)$$

and the effective nucleon masses

$$M_p^* = M + G_S \rho_s + G_{TS} \rho_{s3}, \quad (93)$$

$$M_n^* = M + G_S \rho_s - G_{TS} \rho_{s3}. \quad (94)$$

The kinetic contributions to the energies of the protons and neutrons in nuclear matter are calculated from

$$\mathcal{E}_{kin}^i = \frac{2}{(2\pi)^3} \int_{|k| \leq k_f^i} d^3 k \sqrt{k^2 + (M_i^*)^2} = \frac{1}{4} [3\tilde{E}_i \rho_i + M_i^* \rho_s^i] \quad i = \{p, n\}. \quad (95)$$

Note that *rearrangement* contributions appear explicitly in the expression for the pressure, whereas in the energy density, such contributions are implicit through the specific density dependence of $G_V(\hat{\rho})$.

4.3 QCD constraints

We proceed now with a central theme of this section: establishing connections between the density-dependent point couplings in the Lagrangian (58) and constraints from QCD. Two key features of low-energy, non-perturbative QCD are at the origin of this discussion: the presence of a non-trivial vacuum characterized by strong condensates and the important role of pionic fluctuations governing the low-energy, long wavelength dynamics according to the rules imposed by spontaneously broken chiral symmetry. Our basic conjecture is, consequently, that the nucleon isoscalar self-energies (79) and (82) arise primarily through changes in the quark condensate and in the quark density at finite baryon density, together with chiral (pionic) fluctuations induced by one- and two-pion exchange interactions.

A. In-medium QCD sum rules

QCD sum rules combine dispersion relation methods with operator product expansion techniques in the analysis of correlations functions. When applied to the nucleon, the starting point is a suitably chosen 3-quark operator $J_N(x)$ which carries nucleon quantum numbers. The correlation function

$$\Pi(q^2) = i \int d^4x e^{iq \cdot x} \langle \mathcal{T} J_N(x) \bar{J}_N(0) \rangle \quad (96)$$

has a pole structure which determines the nucleon mass in the presence of the (non-perturbative) QCD vacuum. That same correlation function can be written in terms of the operator product expansion,

$$\Pi(q^2) = \sum_n C_n(q^2) \langle \hat{O}_n \rangle, \quad (97)$$

with vacuum expectation values of local operators \hat{O}_n constructed from quark and gluon fields and organised according to their (mass) dimensions. The operators of lowest non-trivial dimension, $d = 4$, are $m_q \bar{q}q$ and $G_{\mu\nu}G^{\mu\nu}$. The next higher ones include four-quark operators and combinations of quark and gluon fields.

Now, for sufficiently large spacelike $Q^2 = -q^2 > 0$, the coefficients $C_n(q^2)$, called Wilson coefficients, decrease as inverse powers of Q^2 with each of the higher dimensional operators to which they are attached. One can then apply QCD perturbation theory to calculate the C_n . The next step is to match $\Pi(-Q^2)$ with its dispersion relation representation and apply a differential operation, the so-called Borel transform, to improve convergence properties. When this matching is performed, the leading order result for the nucleon mass in vacuum is Ioffe's formula (13).

Applications of QCD sum at finite baryon density ρ proceed in an analogous way, except that now operators such as $q^\dagger q$ also have non-vanishing ground state expectation values: $\langle q^\dagger q \rangle_\rho = 3\rho/2$. In addition, the vacuum condensates vary with increasing density. Thus in-medium QCD sum rules relate the changes of the scalar quark condensate and the quark density at finite baryon density, with the isoscalar scalar and vector self-energies of a nucleon in the nuclear medium. In leading order which should be valid at densities below and around saturated nuclear matter, the

condensate part, $\Sigma_S^{(0)}$, of the scalar self-energy is expressed in terms of the density dependent chiral condensate as follows [6, 7, 8]:

$$\Sigma_S^{(0)} = -\frac{8\pi^2}{\Lambda_B^2} [\langle \bar{q}q \rangle_\rho - \langle \bar{q}q \rangle_0] = -\frac{8\pi^2}{\Lambda_B^2} \frac{\sigma_N}{m_u + m_d} \rho_s, \quad (98)$$

with $\rho_s = \langle \bar{\Psi}\Psi \rangle$. We have used Eq.(40) together with the GOR relation (11). The chiral vacuum condensate $\langle \bar{q}q \rangle_0$ as a measure of spontaneous chiral symmetry breaking in QCD is given in Eq.(12). The difference between the vacuum condensate $\langle \bar{q}q \rangle_0$ and the one at finite density involves the nucleon sigma term, $\sigma_N \sim \langle N | m_q \bar{q}q | N \rangle$, to this order. The Borel mass scale $\Lambda_B \approx 1\text{GeV}$ roughly separates perturbative and non-perturbative domains in the QCD sum rule analysis.

To the same order in the condensates with lowest dimension, the resulting time component of the isoscalar vector self-energy is

$$\Sigma_V^{(0)} = \frac{64\pi^2}{3\Lambda_B^2} \langle q^\dagger q \rangle_\rho = \frac{32\pi^2}{\Lambda_B^2} \rho. \quad (99)$$

It reflects the repulsive density-density correlations associated with the time component of the quark baryon current, $\bar{q}\gamma^\mu q$. Note that, as pointed out in Ref.[6], the ratio

$$\frac{\Sigma_S^{(0)}}{\Sigma_V^{(0)}} = -\frac{\sigma_N}{4(m_u + m_d)} \frac{\rho_s}{\rho} \quad (100)$$

is approximately equal to -1 for typical values of the nucleon sigma term σ_N and the current quark masses $m_{u,d}$, and around nuclear matter saturation density where $\rho_s \simeq \rho$ (as an example, take $\sigma_N \simeq 50$ MeV and $m_u + m_d \simeq 12$ MeV at a scale of 1 GeV).

Identifying the free nucleon mass at $\rho = 0$ according to Ioffe's formula (13), $M = -\frac{8\pi^2}{\Lambda_B^2} \langle \bar{q}q \rangle_0$, one finds

$$\Sigma_S^{(0)}(\rho) = M^*(\rho) - M = -\frac{\sigma_N M}{m_\pi^2 f_\pi^2} \rho_s \quad (101)$$

and

$$\Sigma_V^{(0)}(\rho) = \frac{4(m_u + m_d)M}{m_\pi^2 f_\pi^2} \rho, \quad (102)$$

with the quark masses $m_{u,d}$ to be taken at a renormalization scale $\mu \simeq \Lambda_B \simeq 4\pi f_\pi \simeq 1$ GeV.

Given these self-energies arising from the condensate background, the corresponding equivalent point-coupling strengths $G_{S,V}^{(0)}$ are simply identified through the relations

$$\Sigma_S^{(0)} = G_S^{(0)} \rho_s \quad (103)$$

and

$$\Sigma_V^{(0)} = G_V^{(0)} \rho \quad (104)$$

in mean field approximation. To this order, the couplings $G_{S,V}^{(0)}$ are density independent. Eq.(101) implies (identifying M with the free nucleon mass):

$$\Sigma_S^{(0)} \simeq -350 \text{ MeV} \frac{\sigma_N}{50 \text{ MeV}} \frac{\rho_s}{\rho_0}. \quad (105)$$

Evidently, the leading-order in-medium change of the chiral condensate is a source of a strong, attractive scalar field which acts on the nucleon in such a way as to reduce its mass in nuclear matter by more than 1/3 of its vacuum value as already anticipated in Eq.(42). Using (103) one estimates:

$$G_S^{(0)} \simeq -11 \text{ fm}^2 \frac{\sigma_N}{50 \text{ MeV}} \quad \text{at } \rho_s \simeq \rho_0 = 0.16 \text{ fm}^{-3}. \quad (106)$$

A correspondingly smaller value of $G_S^{(0)}$ would result if only a fraction of the nucleon mass M is associated with the chiral condensate, leaving room for non-leading contributions from higher dimensional condensates. The QCD sum rules suggest that the ratio of the condensate scalar and vector self-energies is close to -1 , so one expects roughly $G_V^{(0)} \simeq -G_S^{(0)}$.

One should note of course that the QCD sum rule constraints implied by Eqs.(101, 102) and by the ratio (100) are not very accurate at a quantitative level. The leading-order Ioffe formula on which Eq.(101) relies has corrections from condensates of higher dimension which are not well under control. The estimated error in the ratio $\Sigma_S^{(0)}/\Sigma_V^{(0)} \simeq -1$ is about 20%, given the uncertainties in the values of σ_N and $m_u + m_d$. Nevertheless, the constraints implied by Eq.(100) give important hints for further orientation.

B. Pionic fluctuations: self-energies from in-medium chiral perturbation theory

The second essential ingredient is the contribution to the nucleon self-energies from chiral fluctuations related to pion-exchange processes (primarily two-pion exchange interactions, with small corrections from one-pion-exchange Fock terms). The corresponding density dependent point-coupling strengths, denoted by $G_{S,V}^{(\pi)}(\rho)$ etc., are calculated using in-medium chiral perturbation theory..

In Section 3 we have shown how the nuclear matter equation of state can be calculated using in-medium chiral perturbation theory up to three loop order in the energy density, expanded in powers of the Fermi momentum k_f (modulo functions of k_f/m_π). The empirical saturation point, the nuclear matter incompressibility, and the asymmetry energy at saturation can be well reproduced at order $\mathcal{O}(k_f^5)$ in the chiral expansion with just one single high-momentum cutoff scale which parametrizes short-distance physics. In this approach the nuclear matter saturation mechanism is entirely determined by the interplay between attraction from two-pion exchange processes and the stabilizing effects of the Pauli principle.

The density dependence of the strength parameters $G^{(\pi)}(\rho)$ originating from pionic (chiral) fluctuations is calculated by equating the isoscalar-scalar, the isoscalar-vector, the isovector-scalar, and the isovector-vector self-energies (79-83) in the single-nucleon Dirac equation (78) with those calculated using in-medium chiral perturbation theory:

$$G_S^{(\pi)} \rho_s = \Sigma_S^{\text{CHPT}}(k_f, \rho), \quad (107)$$

$$G_V^{(\pi)} \rho + \Sigma_r^{(\pi)} = \Sigma_V^{\text{CHPT}}(k_f, \rho), \quad (108)$$

$$G_{TS}^{(\pi)} \rho_{s3} = \Sigma_{TS}^{\text{CHPT}}(k_f, \rho), \quad (109)$$

$$G_{TV}^{(\pi)} \rho_3 = \Sigma_{TV}^{\text{CHPT}}(k_f, \rho), \quad (110)$$

with

$$\Sigma_r^{(\pi)} = \frac{1}{2} \frac{\partial G_S^{(\pi)}}{\partial \rho} \rho_s^2 + \frac{1}{2} \frac{\partial G_V^{(\pi)}}{\partial \rho} \rho^2 + \frac{1}{2} \frac{\partial G_{TS}^{(\pi)}}{\partial \rho} \rho_{s3}^2 + \frac{1}{2} \frac{\partial G_{TV}^{(\pi)}}{\partial \rho} \rho_3^2. \quad (111)$$

The equations of state of symmetric and asymmetric nuclear matter calculated in CHPT give, via the Hugenholtz - van Hove theorem, the sums $U_{(T)}(k_f, k_f) = \Sigma_{(T)S}^{\text{CHPT}}(k_f, \rho) + \Sigma_{(T)V}^{\text{CHPT}}(k_f, \rho)$ of the scalar and vector nucleon self-energies in the isoscalar and isovector channels at the Fermi surface $p = k_f$ up to two-loop order, generated by chiral one- and two-pion exchange [10]. The differences $\Sigma_{(T)S}^{\text{CHPT}}(k_f, \rho) - \Sigma_{(T)V}^{\text{CHPT}}(k_f, \rho)$ are calculated from the same pion-exchange diagrams via charge conjugation (formally evaluating the anti-nucleon single particle potential in nuclear matter). Following a procedure similar to the determination of the nucleon-meson vertices of relativistic mean-field models from Dirac-Brueckner calculations [49], we neglect the momentum dependence of $\Sigma_{(T)S,V}^{\text{CHPT}}(p, \rho)$ and take their values at the Fermi surface $p = k_f$. A polynomial fit up to order k_f^5 is performed, and all four CHPT self-energies have the same functional form,

$$\begin{aligned} \Sigma^{\text{CHPT}}(k_f, \lambda) = & \left[c_{30} + c_{31}\lambda + c_{32}\lambda^2 + c_{3L} \ln \frac{m_\pi}{4\pi f_\pi \lambda} \right] \frac{k_f^3}{M^2} \\ & + c_{40} \frac{k_f^4}{M^3} + \left[c_{50} + c_{5L} \ln \frac{m_\pi}{4\pi f_\pi \lambda} \right] \frac{k_f^5}{M^4}, \end{aligned} \quad (112)$$

where the dimensionless parameter λ is related to the momentum cut-off scale by $\Lambda = 2\pi f_\pi \lambda$, and $f_\pi = 92.4$ MeV denotes the pion decay constant. The cut-off parameter $\Lambda \simeq 0.65$ GeV that has been adjusted to the nuclear matter saturation in Ref.[9], corresponds to $\lambda = 1.113$. In order to determine the density dependence of the couplings from Eqs. (107-110), the CHPT self-energies are re-expressed in terms of the baryon density $\rho = 2k_f^3/3\pi^2$:

$$\Sigma_S^{\text{CHPT}}(k_f, \rho) = (c_{s1} + c_{s2}\rho^{\frac{1}{3}} + c_{s3}\rho^{\frac{2}{3}})\rho, \quad (113)$$

$$\Sigma_V^{\text{CHPT}}(k_f, \rho) = (c_{v1} + c_{v2}\rho^{\frac{1}{3}} + c_{v3}\rho^{\frac{2}{3}})\rho, \quad (114)$$

$$\Sigma_{TS}^{\text{CHPT}}(k_f, \rho) = (c_{ts1} + c_{ts2}\rho^{\frac{1}{3}} + c_{ts3}\rho^{\frac{2}{3}})\rho_3, \quad (115)$$

$$\Sigma_{TV}^{\text{CHPT}}(k_f, \rho) = (c_{tv1} + c_{tv2}\rho^{\frac{1}{3}} + c_{tv3}\rho^{\frac{2}{3}})\rho_3. \quad (116)$$

The resulting expressions for the density dependent couplings of the pionic fluctuation terms are⁸

$$G_S^{(\pi)} = c_{s1} + c_{s2}\rho^{\frac{1}{3}} + c_{s3}\rho^{\frac{2}{3}}, \quad (117)$$

$$G_V^{(\pi)} = \bar{c}_{v1} + \bar{c}_{v2}\rho^{\frac{1}{3}} + \bar{c}_{v3}\rho^{\frac{2}{3}} \quad \begin{cases} \bar{c}_{v1} = c_{v1} \\ \bar{c}_{v2} = (6c_{v2} - c_{s2} - \delta^2(c_{ts2} + c_{tv2}))/7 \\ \bar{c}_{v3} = (3c_{v3} - c_{s3} - \delta^2(c_{ts3} + c_{tv3}))/4 \end{cases}, \quad (118)$$

$$G_{TS}^{(\pi)} = c_{ts1} + c_{ts2}\rho^{\frac{1}{3}} + c_{ts3}\rho^{\frac{2}{3}}, \quad (119)$$

$$G_{TV}^{(\pi)} = c_{tv1} + c_{tv2}\rho^{\frac{1}{3}} + c_{tv3}\rho^{\frac{2}{3}}, \quad (120)$$

where $\delta = (\rho_p - \rho_n)/(\rho_p + \rho_n)$. For $\lambda = 1.113$, the coefficients of the expansion of the CHPT self-energies in powers of the baryon density Eqs.(113-116) are given in Table 1.

⁸ small differences between ρ_s and ρ at nuclear matter densities are neglected here

Table 1. The coefficients of the expansion of the in-medium CHPT self energies (113) – (116) in powers of the baryon density, for the value of the cut-off parameter $\Lambda = 646.3$ MeV. In this case we assumed $N = Z$, neglecting isovector contributions.

c_{s1}	-2.805 fm^2	c_{ts1}	-0.373 fm^2
c_{s2}	2.738 fm^3	c_{ts2}	0.251 fm^3
c_{s3}	1.346 fm^4	c_{ts3}	0.387 fm^4
c_{v1}	-2.718 fm^2	c_{tv1}	-0.562 fm^2
c_{v2}	2.841 fm^3	c_{tv2}	0.207 fm^3
c_{v3}	1.325 fm^4	c_{tv3}	0.398 fm^4

Combining now the effects from leading order QCD condensates and pionic fluctuations, the strength parameters of the isoscalar four-fermion interaction terms in the Lagrangian (58) are:

$$G_{S,V}(\rho) = G_{S,V}^{(0)} + G_{S,V}^{(\pi)}(\rho) . \quad (121)$$

For the isovector channels we assume that only pionic (chiral) fluctuations contribute.

C. Corrections of higher order

Up to this point the nucleon self-energies are evaluated at chiral two-loop level including terms of order k_f^5 . At order k_f^6 ($\propto \rho^2$), several additional effects appear. First, condensates of higher dimension enter, such as $\langle \bar{q}\Gamma q\bar{q}\Gamma q \rangle$, $\langle q^\dagger q \rangle^2$. Their detailed in-medium dependence is difficult to estimate. Secondly, four-loop CHPT contributions to the energy density (three-loop in the self-energies) introduce genuine 3-body interactions. All those effects combine to produce the $\mathcal{O}(k_f^6)$ correction in the energy per particle. Our conjecture is that these terms should be subleading in the k_f -expansion. In estimating those contributions, we will take a pragmatic point of view. Given the density-independent leading condensate terms $G^{(0)}$ and the CHPT couplings $G^{(\pi)}(\rho)$ evaluated to $\mathcal{O}(k_f^5) \propto \rho^{\frac{2}{3}}$, we generalize

$$G(\rho) = G^{(0)} + G^{(\pi)}(\rho) + \delta G^{(1)}(\rho) , \quad (122)$$

adding terms $\delta G^{(1)} = g^{(1)}\rho$ and let the constant $g^{(1)}$ be determined by a least squares fit to properties of nuclear matter and finite nuclei. At first sight, the corrections $\delta G_S^{(1)}$, $\delta G_V^{(1)}$, etc... would then introduce several additional parameters, undermining our strategy to keep the number of freely adjustable fine-tuning constants as small as possible. For the scalar self-energy a primary uncertainty arises from the four-quark condensate. It is common practice to approximate $\langle qq\bar{q}q \rangle$ assuming factorization into the form $\langle \bar{q}q \rangle^2$, which introduces potentially large and uncontrolled errors as discussed in detail in Ref. [8]. While the in-medium values of condensates such as $\langle \bar{q}\Gamma q\bar{q}\Gamma q \rangle$ are thus not well determined, it nevertheless appears

that only a weak or moderate density dependence of these condensates is consistent with known nuclear phenomenology. We do not have to be much concerned about this issue here because our *explicit* treatment of scalar $\pi\pi$ fluctuations (up to order k_f^5 in the energy density) removes at least part of such uncertainties. What we can conclude from this calculation is that factorization of the four-quark condensates, assuming ground state dominance, is not justified since the QCD ground state strongly couples to the scalar two-pion continuum via the operator $\bar{q}q$.

So as a first option, we assume that the only non-vanishing $\delta G^{(1)}$ is $\delta G_V^{(1)} = g_V^{(1)} \rho$, and determine the constant $g_V^{(1)}$. Note that this $\delta G^{(1)}$ produces a self-energy contribution $\delta\Sigma^{(1)} \propto \rho^2$ which acts like a three-body force.

4.4 Nuclear matter, part III

We return now to the calculation of the nuclear matter equation of state (EOS), using the relativistic point-coupling model with QCD-constrained input as outlined in the previous sections. These calculations are performed in three steps.

i) In the first step we follow the implicit assumption made in Ref.[9] and in Section 3, namely that $\Sigma_S^{(0)} = -\Sigma_V^{(0)}$ in nuclear matter, and ignore the contribution of the condensate background self-energies. The point-coupling model, with the density dependence of the strength parameters determined by pionic (chiral) fluctuations, nicely reproduces the nuclear matter EOS calculated previously using in-medium CHPT: the binding energy per particle, the saturation density, the compression modulus, and the asymmetry energy. Small differences arise mainly because in the mapping of the CHPT nucleon self-energies on the self-energies of the point coupling model in Eqs. (107-110), the momentum dependence of the former has been frozen to the values at the Fermi momentum. This is a well known problem that arises also in the determination of the meson-nucleon in-medium vertices from Dirac-Brueckner calculations of nucleon self-energies in nuclear matter [49].

At very low-densities, the CHPT equation of state cannot reproduce realistic calculations of E/A , for obvious reasons. The low density limit of the energy per particle is not given by a free Fermi gas of nucleons. Proton-neutron pairs coalesce to form deuteron bound-states, an entirely non-perturbative phenomenon that cannot be handled at any order of a perturbative approach. The low-density limit of E/A approaches a constant as $k_f \rightarrow 0$, namely one half of the deuteron binding energy. The effect of this shift is marginal, however, for the bulk of nuclear matter around saturation density.

ii) The next step includes the contributions of the condensate background self-energies, $\Sigma_{S,V}^{(0)}$, in the isoscalar-scalar and isoscalar-vector channels. In Ref.[12] we have shown that, even though to first approximation the condensate potentials do not play a role in the saturation mechanism, they are indeed essential for the description of ground-state properties of finite nuclei.

At this stage we first treat both $G_S^{(0)}$ and $G_V^{(0)}$ as independent parameters, irrespective of the QCD sum rule constraint (100). The three parameters: $G_S^{(0)}$, $G_V^{(0)}$ and Λ (the CHPT cutoff scale), are then adjusted to reproduce “empirical” nuclear matter properties: $E/A = -16$ MeV (5%), $\rho_0 = 0.153$ fm $^{-3}$ (10%), the compression modulus $K_0 = 250$ MeV (10%), and the asymmetry energy $A_0 = 33$ MeV (10%). The values in parentheses refer to the error bars used in the fitting procedure.

Table 2. Nuclear matter saturation properties calculated in the relativistic point-coupling model constrained by in-medium QCD sum rules and chiral perturbation theory. In addition to the chiral one- and two-pion exchange contribution to the density dependence of the coupling parameters, the nuclear matter EOS shown in the first row incorporates the isoscalar condensate background nucleon self-energies linear in the corresponding densities. The EOS displayed in the second row is calculated by including also the non-linear “3-body” contribution (proportional to ρ^2) in the isoscalar vector condensate self-energy.

	E/A[MeV]	ρ_0 [fm $^{-3}$]	K_0 [MeV]	M^*/M	A_0 [MeV]
LINEAR	-15.97	0.148	283	0.753	45.3
NON-LINEAR	-15.76	0.151	332	0.620	30.2

The corresponding *least-squares fit* yields $G_S^{(0)} = -7 \text{ fm}^2$, $G_V^{(0)} = 7 \text{ fm}^2$, and $\Lambda = 685 \text{ MeV}$. The result is shown in Fig. 4 (EOS of isospin symmetric nuclear matter in comparison with the one calculated exclusively from chiral pion-exchange) and in the first row of Table 2. The EOS so obtained is not yet satisfactory. The asymmetry energy A_0 at saturation is too high, and the values of $G_S^{(0)}$ and $G_V^{(0)}$ are smaller than the leading order QCD sum rule estimate (106). This results in the relatively large Dirac effective mass $M^*/M = 0.75$. A high Dirac mass in turn indicates that the effective single-nucleon spin-orbit potential is too weak to reproduce the empirical energy spacings between spin-orbit partner states in finite nuclei. Stronger background scalar and vector fields are required in order to drive the large spin-orbit splittings in finite nuclei.

Notice however that, even though $G_S^{(0)}$ and $G_V^{(0)}$ were varied *independently*, the minimization procedure chooses to balance the contributions from the corresponding large scalar and vector self-energies, such that their sum tends to vanish: there is already sufficient binding from pionic fluctuations alone, so that even the unconstrained fit prefers $\Sigma_S^{(0)} = -\Sigma_V^{(0)}$ for the condensate potentials. This remarkable feature prevails as we now proceed with fine-tuning improvements.

iii) The third step incorporates in addition the higher-order correction $\delta G_V^{(1)} = g_V^{(1)} \rho$, see Eq.(122). For $G_S^{(0)} = -12 \text{ fm}^2$, $G_V^{(0)} = 11 \text{ fm}^2$, $g_V^{(1)} = -3.9 \text{ fm}^5$ and $\Lambda = 600 \text{ MeV}$, determined in a *least-squares fit* to the “empirical” nuclear matter input, the EOS resulting is displayed in Fig. 4 and the nuclear matter properties at saturation are listed in the second row of Table 2. This nuclear matter EOS is actually quite satisfactory, with realistic values of the binding energy, saturation density, asymmetry energy at saturation, and a low effective Dirac mass. The only exception is a relatively large nuclear matter incompressibility. It could be cured by introducing a ρ^3 term in the expansion of the self-energies, but we prefer not to invoke additional fine-tuning parameters at this level of the discussion.

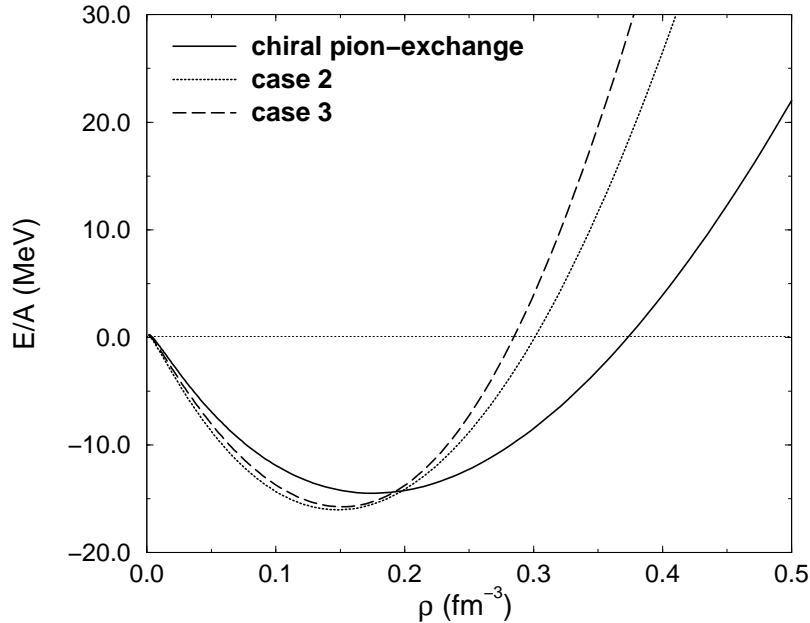


Fig. 4. Binding energy per nucleon for symmetric nuclear matter as a function of the baryon density, calculated from chiral one- and two-pion exchange between nucleons (case 1, solid curve), by adding the isoscalar condensate background nucleon self-energies linear in the corresponding densities, with $G_V^{(0)} = -G_S^{(0)} = 7 \text{ fm}^2$ (case 2, dotted curve), and finally by including also the non-linear contribution $g_V^{(1)} \rho^2$ to the isoscalar vector condensate self-energy, with $G_V^{(0)} = 11 \text{ fm}^2$, $G_S^{(0)} = -12 \text{ fm}^2$ (case 3, dashed curve).

The resulting couplings $G_{S,V}^{(0)}$ of the condensate background fields are remarkably close to the prediction (106) of the leading order in-medium QCD sum rules. The scalar and the vector “condensate” self-energies $\Sigma_S^{(0)} = G_S^{(0)} \rho_s$ and $\Sigma_V^{(0)} = G_V^{(0)} \rho$ follow the expectation $\Sigma_S^{(0)} \simeq -\Sigma_V^{(0)}$ to within 5% at saturation density, even without this condition being pre-imposed. The large isoscalar condensate background self-energies in turn lead to a relatively low effective Dirac mass, crucial for the empirical spin-orbit splittings in finite nuclei. Finally, the cut-off $\Lambda = 600 \text{ MeV}$ differs by less than 10 % from the value (646 MeV) obtained when the nuclear matter EOS results exclusively from one- and two-pion exchange between nucleons [9]. The $\delta G_V^{(1)} = g_V^{(1)} \rho$ term is relatively small: at saturation density, $\delta G_V^{(1)} / G_V^{(0)} \simeq 0.05$. Splitting $\delta G^{(1)}$ between scalar and vector parts (e.g. by choosing $\delta G_V^{(1)} \simeq \delta G_S^{(1)} \simeq -2 \text{ fm}^{-5}$) would induce only marginal changes.

4.5 Comparison with Dirac-Brueckner G-matrix theory

At this point it is instructive to compare the density-dependence of our self-energies $\Sigma_{S,V}(\rho)$ with that of the scalar and the vector self-energies resulting from Dirac-Brueckner G-matrix calculations which start from realistic NN-interactions V_{NN} . Brueckner calculations iterate V_{NN} to all orders in the ladder approximation, keeping track of Pauli exclusion principle effects on intermediate NN states. In addition, the Dirac-Brueckner approach takes into account the lower components of the relativistic (Dirac) wave functions of the nucleons, so that the density dependent nucleon self-energies resulting from such calculations separate into Lorentz scalar and vector parts.

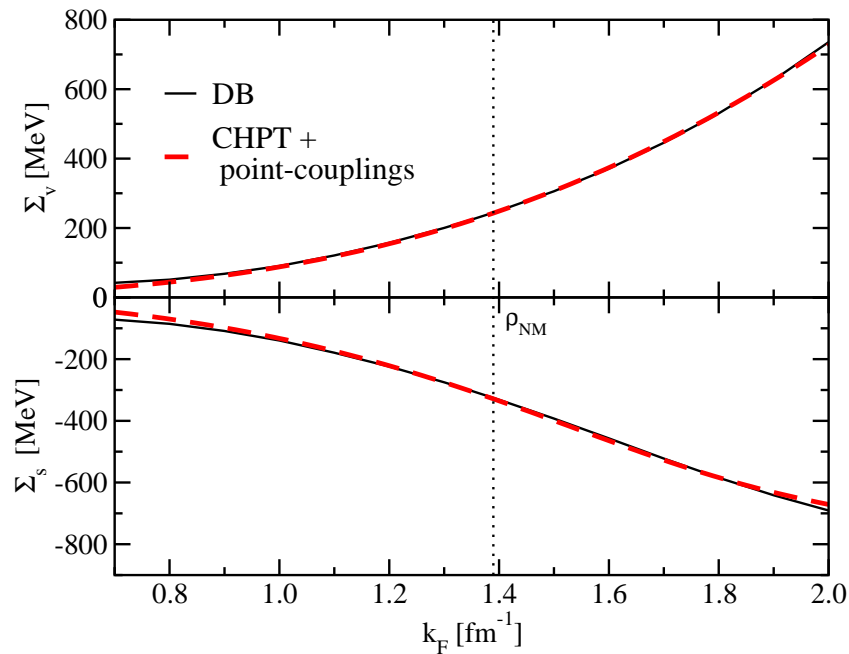


Fig. 5. Comparison of the k_f -dependencies of isoscalar vector and scalar self-energies resulting from a Dirac-Brueckner calculation (solid lines: DB [52]) with the self-energies generated from in-medium chiral perturbation theory (dashed lines: CHPT + point-couplings) up to 3-loop order in the energy density. (We thank Paolo Finelli for preparing this figure.)

We refer here explicitly to a calculation, reported in Ref. [52], which uses the Bonn A potential. With this potential, the nuclear matter saturation density comes out somewhat too high ($\rho_{sat} \simeq 0.185 \text{ fm}^{-3}$), higher than the one of our best fit. In

order to perform a meaningful comparison, simulating this larger saturation density in our approach requires weakening the condensate mean fields $\Sigma_{S,V}^{(0)}$ by about 25 %, but with no changes in the pionic terms $\Sigma_{S,V}^{(\pi)}$. After this readjustment the difference in the k_f -dependences between our Σ_S and Σ_V and those resulting from the Dirac-Brueckner calculation is less than 10 % over the entire range of densities from $0.5\rho_0$ to $2.5\rho_0$ (see Fig. 5). This is a remarkable observation: it appears that in-medium chiral perturbation theory at two-loop order, with a cut-off scale $\Lambda \simeq 0.6$ GeV that converts unresolved short-distance dynamics at momenta beyond Λ effectively into contact terms, generates quantitatively similar in-medium nucleon self energies as a full Dirac-Brueckner calculation, when requiring that both approaches reproduce the same nuclear matter saturation point. The reasoning behind this observation can presumably be traced back to the separation of scales at work, a key element of chiral effective field theory on which our approach is based. One- and two-pion exchange in-medium dynamics at momentum scales comparable to k_f must be treated explicitly. Our in-medium CHPT approach includes all terms (ladders and others) to three-loop order in the energy density, a prominent one being iterated one-pion exchange. The non-trivial k_f dependence in the self-energies (beyond “trivial” order k_f^3) reflects the action of the Pauli principle in these processes. Such features are also present in leading orders of the Brueckner ladder summation which includes, for example, Pauli effects on iterated one-pion exchange. On the other hand, the iteration of short-distance interactions to all orders involves intermediate momenta much larger than k_f and generates effectively the same self-energy pieces (proportional to density ρ) as a suitably chosen contact interaction: the infinite ladder summation of short-distance interactions can simply be subsumed in a contact term reflecting the high-momentum scale Λ . The reasoning here has a close correspondence to related studies in Ref. [53].

4.6 Intermediate summary and discussion

While the quantitative details for the terms contributing to the scalar and vector self-energies can be reconstructed from the tables and figures that we have included in this section, it is instructive to observe systematic trends in these self-energies when expanded in powers of k_f (or equivalently, in powers of $\rho^{\frac{1}{3}}$). We focus on symmetric nuclear matter and write

$$\Sigma_{S,V} = \Sigma_{S,V}^{(0)} + \Sigma_{S,V}^{(\pi)} + \delta\Sigma_{S,V} , \quad (123)$$

combining the leading condensate terms $\Sigma_{S,V}^{(0)}$, the chiral (pionic) terms $\Sigma_{S,V}^{(\pi)}$ calculated to order k_f^5 , and possible corrections of higher order summarized in $\delta\Sigma_{S,V}$. We introduce the saturation density $\rho_0 = 0.16 \text{ fm}^{-3}$ as a convenient scale and write the condensate terms as

$$\Sigma_S^{(0)}(\rho) \simeq -0.35 \text{ GeV} \frac{|G_S^{(0)}|}{11 \text{ fm}^2} \left(\frac{\rho_s}{\rho_0} \right) , \quad (124)$$

$$\Sigma_V^{(0)}(\rho) \simeq +0.35 \text{ GeV} \frac{|G_V^{(0)}|}{11 \text{ fm}^2} \left(\frac{\rho}{\rho_0} \right) . \quad (125)$$

We note that with $|G_S^{(0)}|$ chosen less than 5% larger than $G_V^{(0)}$, this just compensates for the difference between the baryon density ρ and the scalar density $\rho_s < \rho$

such that $\Sigma_S^{(0)} \simeq -\Sigma_V^{(0)}$ results at $\rho = \rho_0$. The “best-fit” values $G_S^{(0)} \simeq -12 \text{ fm}^2$ and $G_V^{(0)} \simeq +11 \text{ fm}^2$ are thus perfectly consistent with QCD sum rule expectations: a non-trivial result. The pionic fluctuations from one- and two-pion exchange processes have the following approximate pattern:

$$\Sigma_{S,V}^{(\pi)}(\rho) \simeq -75 \text{ MeV} \left(\frac{\rho}{\rho_0} \right) \left[1 + d_1 \left(\frac{\rho}{\rho_0} \right)^{\frac{1}{3}} + d_2 \left(\frac{\rho}{\rho_0} \right)^{\frac{2}{3}} \right], \quad (126)$$

where d_1 varies between -0.61 (scalar) and -0.65 (vector) and $d_2 \simeq -0.17$ for both cases. Finally, the higher order corrections are summarized as

$$\delta\Sigma_S + \delta\Sigma_V \simeq -20 \text{ MeV} \left(\frac{\rho}{\rho_0} \right)^2, \quad (127)$$

where the detailed decomposition into scalar and vector part turns out not to be relevant.

The leading attraction at $\mathcal{O}(k_f^3)$ in $\Sigma_{S,V}^{(\pi)}$ depends on the cut-off scale $\Lambda \equiv 2\pi f_\pi \lambda$ which separates “active” two-pion exchange dynamics at long and intermediate distances from short-distance (high momentum) dynamics. Details at short distance scales (related to the intrinsic structure of the nucleons and their short-range interactions) are not resolved as long as the Fermi momentum k_f is small compared to the chiral symmetry breaking scale, $4\pi f_\pi$. The unresolved short-distance information can then be translated into an equivalent (density-independent) four-point vertex which generates self-energy terms linear in the density at the mean-field level.

5 Finite Nuclei

In this section the relativistic nuclear point-coupling model, constrained by in-medium QCD sum rules and chiral perturbation theory, is applied in calculations of ground state properties of finite nuclei. In the mean-field approximation the ground state of a nucleus with A nucleons is represented by the antisymmetrized product of the lowest occupied single-nucleon stationary solutions of the Dirac equation (63). The calculation is self-consistent in the sense that the nucleon self-energies are functions of nucleon densities and currents, calculated from the solutions of Eq. (63). The mean-field approach to nuclear structure represents an approximate implementation of Kohn-Sham density functional theory (DFT) [54, 55, 56], which is successfully employed in the treatment of the quantum many-body problem in atomic, molecular and condensed matter physics. At the basis of the DFT approach are energy functionals of the ground-state density. In relativistic mean-field models these become functionals of the ground-state scalar density and of the baryon current. The scalar and vector self-energies play the role of local relativistic Kohn-Sham potentials [1, 5]. The mean-field models approximate the exact energy functional, which includes all higher-order correlations, by powers and gradients of fields or densities, with the truncation determined by power counting [5].

5.1 Ground state energy

In this lecture we only consider spherical even-even nuclei. Because of time-reversal invariance the spatial components of the four-currents vanish, and the nucleon self-energies (reduced to the time component Σ^0 of the vector terms Σ^μ) read:

$$\Sigma^0 = G_V \rho + D_V \Delta \rho - eA^0 \frac{1 + \tau_3}{2}, \quad (128)$$

$$\Sigma_T^0 = G_{TV} \rho_3 + D_{TV} \Delta \rho_3, \quad (129)$$

$$\Sigma_S = G_S \rho_s + D_S \Delta \rho_s, \quad (130)$$

$$\Sigma_{TS} = G_{TS} \rho_{s3} + D_{TS} \Delta \rho_{s3}, \quad (131)$$

$$\Sigma_{rS} = \frac{\partial D_S}{\partial \rho} (\nabla \rho_s) \cdot (\nabla \rho), \quad (132)$$

$$\Sigma_{rTS} = \frac{\partial D_{TS}}{\partial \rho} (\nabla \rho_{s3}) \cdot (\nabla \rho), \quad (133)$$

$$\Sigma_{rT}^0 = \frac{\partial D_{TV}}{\partial \rho} (\nabla \rho_3) \cdot (\nabla \rho), \quad (134)$$

$$\begin{aligned} \Sigma_r^0 = & + \frac{1}{2} \frac{\partial G_S}{\partial \rho} \rho_s^2 - \frac{1}{2} \frac{\partial D_S}{\partial \rho} (\nabla \rho_s) \cdot (\nabla \rho_s) \\ & + \frac{1}{2} \frac{\partial G_V}{\partial \rho} \rho^2 - \frac{1}{2} \frac{\partial D_V}{\partial \rho} (\nabla \rho) \cdot (\nabla \rho) \\ & + \frac{1}{2} \frac{\partial G_{TS}}{\partial \rho} \rho_{s3}^2 - \frac{1}{2} \frac{\partial D_{TS}}{\partial \rho} (\nabla \rho_{s3}) \cdot (\nabla \rho_{s3}) \\ & + \frac{1}{2} \frac{\partial G_{TV}}{\partial \rho} \rho_3^2 - \frac{1}{2} \frac{\partial D_{TV}}{\partial \rho} (\nabla \rho_3) \cdot (\nabla \rho_3) \\ & + \frac{\partial D_V}{\partial \rho} (\nabla \rho) \cdot (\nabla \rho). \end{aligned} \quad (135)$$

In the *mean-field* approximation the isoscalar-scalar, isoscalar-vector, isovector-scalar and isovector-vector ground state densities are calculated from the Dirac wave functions ψ_k of the occupied positive-energy orbits as:

$$\rho_s = \sum_{k=1}^A \bar{\psi}_k \psi_k, \quad (136)$$

$$\rho = \sum_{k=1}^A \psi_k^\dagger \psi_k, \quad (137)$$

$$\rho_{s3} = \sum_{k=1}^A \bar{\psi}_k \tau_3 \psi_k, \quad (138)$$

$$\rho_3 = \sum_{k=1}^A \psi_k^\dagger \tau_3 \psi_k, \quad (139)$$

respectively. The expression for the ground state energy of a nucleus with A nucleons reads:

$$\begin{aligned}
E = \sum_{k=1}^A \epsilon_k - \frac{1}{2} \int d^3x \{ & G_S \rho_s^2 + D_S \rho_s \Delta \rho_s + G_V \rho^2 + D_V \rho \Delta \rho \\
& + G_{TV} \rho_3^2 + D_{TV} \rho_3 \Delta \rho_3 + G_{TS} \rho_{s3}^2 + D_{TS} \rho_{s3} \Delta \rho_{s3} + j^p V_C \\
& + \frac{\partial G_S}{\partial \rho} \rho_s^2 \rho + \frac{\partial G_V}{\partial \rho} \rho^3 + \frac{\partial G_{TV}}{\partial \rho} \rho_3^2 \rho + \frac{\partial G_{TS}}{\partial \rho} \rho_{s3}^2 \rho \\
& - \frac{\partial D_S}{\partial \rho} (\nabla \rho_s) \cdot (\nabla \rho_s) \rho + \frac{\partial D_V}{\partial \rho} (\nabla \rho) \cdot (\nabla \rho) \rho \\
& - \frac{\partial D_{TV}}{\partial \rho} (\nabla \rho_3) \cdot (\nabla \rho_3) \rho - \frac{\partial D_{TS}}{\partial \rho} (\nabla \rho_{s3}) \cdot (\nabla \rho_{s3}) \rho \\
& + 2 \frac{\partial D_S}{\partial \rho} (\nabla \rho_s) \cdot (\nabla \rho) \rho_s + 2 \frac{\partial D_{TV}}{\partial \rho} (\nabla \rho_3) \cdot (\nabla \rho) \rho_3 \\
& + 2 \frac{\partial D_{TS}}{\partial \rho} (\nabla \rho_{s3}) \cdot (\nabla \rho) \rho_{s3} \} , \tag{140}
\end{aligned}$$

where ϵ_k denotes the single-nucleon energies. In addition, for open shell nuclei pairing correlations are included in the simple BCS approximation [57]. After the solution of the self-consistent Dirac equation, the microscopic estimate for the center-of-mass correction

$$E_{cm} = - \frac{\langle P_{cm}^2 \rangle}{2AM} , \tag{141}$$

is subtracted from the total binding energy. Here P_{cm} is the total momentum of the nucleus with A nucleons.

5.2 Surface (derivative) terms

The calculated properties of finite nuclei depend of course on an accurate tuning of coupling parameters. We keep the variational freedom in those parameters at minimum, constraining the density-dependent couplings G_S , G_V , G_{TS} and G_{TV} by in-medium QCD sum rules and explicit chiral perturbation theory calculations of one- and two-pion exchange diagrams, as described in the previous sections. For finite nuclei, fine-tuning of their detailed surface structure will be required, so we must also determine the coupling parameters of the derivative terms: D_S , D_V , D_{TS} and D_{TV} . Dimensional considerations suggest the following ansatz

$$D(\rho) = \frac{G(\rho)}{\mathcal{M}^2} , \tag{142}$$

where \mathcal{M} is a characteristic mass scale for a given spin-isospin channel. There is no deeper reason, however, for the derivative terms to have the same density dependence as the coupling parameters of the four-fermion interactions. The density dependence of $D_i(\rho)$ could, in principle, be derived by CHPT calculations for inhomogeneous nuclear matter. A simpler option, followed here, is to treat the D 's as density-independent adjustable constants. In this case the remaining rearrangement contribution to the vector-self energy becomes, of course, much simpler. As it has been emphasized by Serot and Furnstahl [43], the empirical data set of bulk and single-particle properties of finite nuclei can only constrain six or seven parameters in the general expansion of the effective Lagrangian in powers of the fields and their derivatives. In particular, only one parameter of the derivative terms can

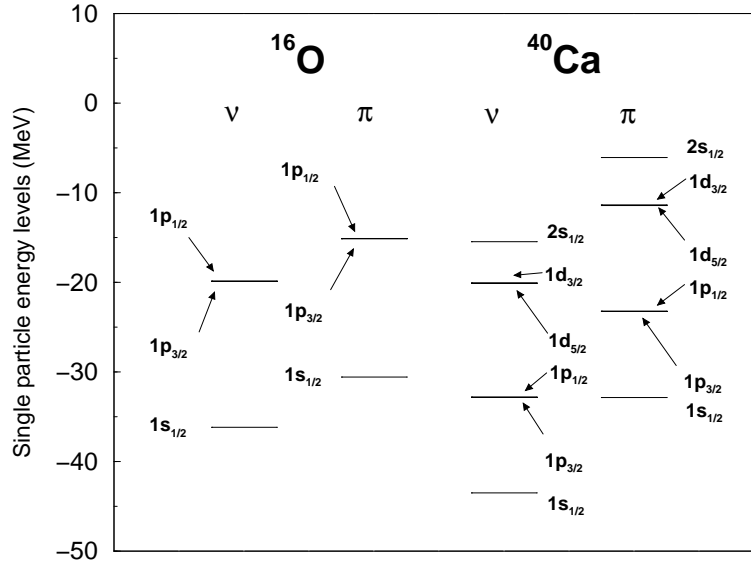


Fig. 6. Neutron and proton single-particle levels in ^{16}O and ^{40}Ca calculated in the relativistic point-coupling model. The density dependent coupling strengths include only the contribution from chiral one- and two-pion exchange between nucleons. (From Ref. [13].)

be determined by the binding energies and radii of spherical nuclei. In the present analysis we therefore set D_V , D_{TS} and D_{TV} equal to zero, and adjust the single remaining surface parameter D_S of the isoscalar-scalar derivative term to properties of light and medium-heavy $N \approx Z$ nuclei. This approximation, which was first used by Serot and Walecka in Ref. [58], implies that the isoscalar-vector, the isovector-scalar and the isovector-vector interactions are considered to be purely contact interactions (no gradient terms).

5.3 Single-particle energies

It is instructive to consider separately the contributions from chiral pion dynamics and condensate background self-energies to properties of finite nuclei. In a first step we have calculated the ground states of ^{16}O and ^{40}Ca using the coupling parameters determined by the nuclear matter EOS of Ref. [9]: $G_S(\rho) = G_S^{(\pi)}(\rho)$, $G_V(\rho) = G_V^{(\pi)}(\rho)$, $G_{TS}(\rho) = G_{TS}^{(\pi)}(\rho)$, $G_{TV}(\rho) = G_{TV}^{(\pi)}(\rho)$, $\Lambda = 646.3$ MeV, while the couplings $G_{S,V}^{(0)}$ to the condensate background fields are set to zero. In this case the nuclear dynamics is completely determined by chiral (pionic) fluctuations. The resulting total binding energies are already within 5–8 % of the experimental values, but the radii of the two nuclei are too small (by about 0.2 fm). This is because the spin-orbit partners ($1p_{3/2}, 1p_{1/2}$) and ($1d_{5/2}, 1d_{3/2}$) are practically degenerate. In

Fig. 6 we display the calculated neutron and proton single-particle levels of ^{16}O and ^{40}Ca . The energies of the degenerate doublets are close to the empirical positions of the centroids of the spin-orbit partner levels, and even the calculated energies of the s -states are realistic. This is an interesting result. Chiral pion dynamics provides the saturation mechanism and binding of nuclear matter, but not the strong spin-orbit force. The inclusion of the isoscalar-scalar derivative term has some effect on the calculated radii but it cannot remove the degeneracy of the spin-orbit doublets.

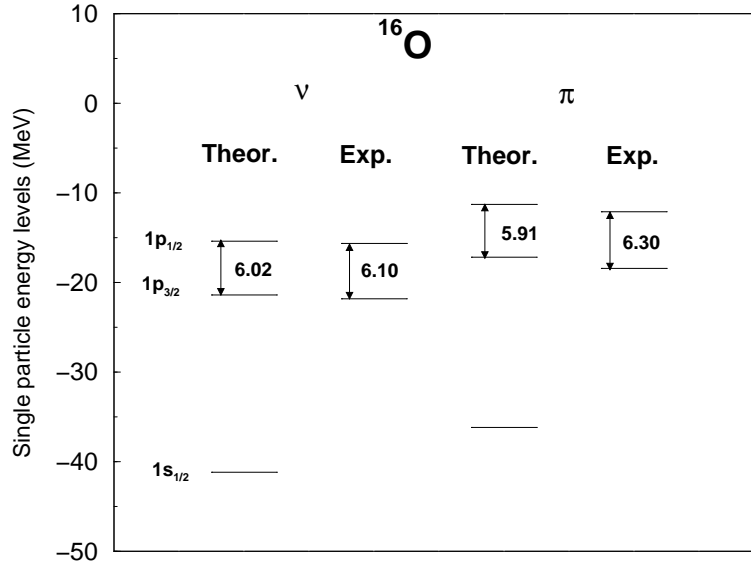


Fig. 7. The neutron and proton single-particle levels in ^{16}O calculated in the relativistic point-coupling model, are shown in comparison with experimental levels. The calculation is performed by including both the contributions of chiral pion-nucleon exchange and of the isoscalar condensate self-energies. (From Ref. [13].)

The spin-orbit potential plays a central role in nuclear structure. It is at the basis of the nuclear shell model, and its inclusion is essential in order to reproduce the experimentally established magic numbers. In non-relativistic models based on the mean-field approximation, the spin-orbit potential is included in a purely phenomenological way, introducing the strength of the spin-orbit interaction as an additional parameter. Its value is usually adjusted to the experimental spin-orbit splittings in spherical nuclei, for example ^{16}O . On the other hand, in the relativistic description of the nuclear many-body problem, the spin-orbit interaction arises naturally from the scalar-vector Lorentz structure of the effective Lagrangian. In the first order approximation, and assuming spherical symmetry, the spin-orbit term of the effective single-nucleon potential can be written as

$$V_{s.o.} = \frac{1}{2M^2} \left(\frac{1}{r} \frac{\partial}{\partial r} V_{ls}(r) \right) \mathbf{l} \cdot \mathbf{s} , \quad (143)$$

where the large spin-orbit potential V_{ls} arises from the difference of the vector and scalar potentials, $V - S \sim 0.7$ GeV [2, 59]. Explicitly,

$$V_{ls} = \frac{M}{M_{eff}} (V - S) . \quad (144)$$

where M_{eff} is an effective mass specified as [2]

$$M_{eff} = M - \frac{1}{2}(V - S) . \quad (145)$$

The isoscalar nucleon self-energies generated by pion exchange are not sufficiently large to produce the empirical effective spin-orbit potential. The degeneracy of spin-orbit doublets is removed by including the isoscalar background self-energies $\Sigma_{S,V}^{(0)}$ that arise through changes in the quark condensate and the quark density at finite baryon density.

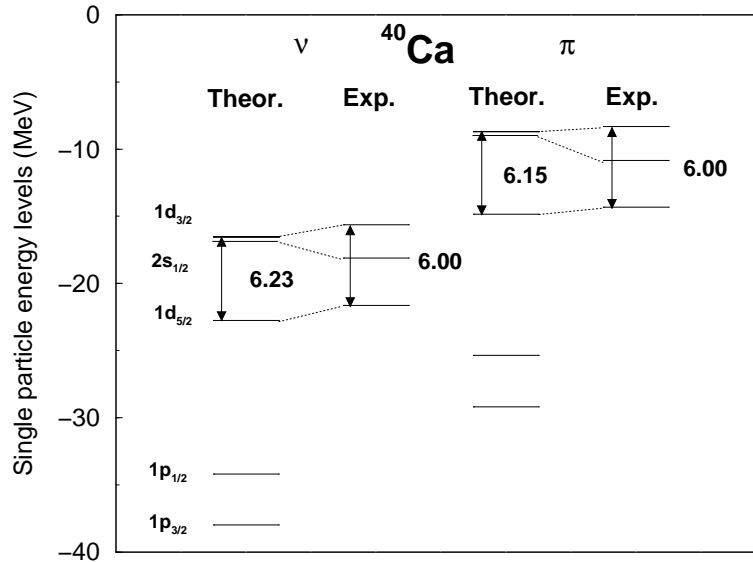


Fig. 8. Same as in Fig. 7, but for ^{40}Ca . (From Ref. [13].)

The effect of including $\Sigma_{S,V}^{(0)}$ is demonstrated in Figs. 7 and 8. In addition to the four parameters ($G_S^{(0)} = -12 \text{ fm}^2$, $G_V^{(0)} = 11 \text{ fm}^2$, $g_V^{(1)} = -3.9 \text{ fm}^5$ and $\Lambda = 600$ MeV) determined by the nuclear matter equation of state, we have adjusted the isoscalar-scalar derivative term: $D_S = -0.713 \text{ fm}^4$. This value of D_S is very close to the ones used in the effective interactions of the standard relativistic point-coupling

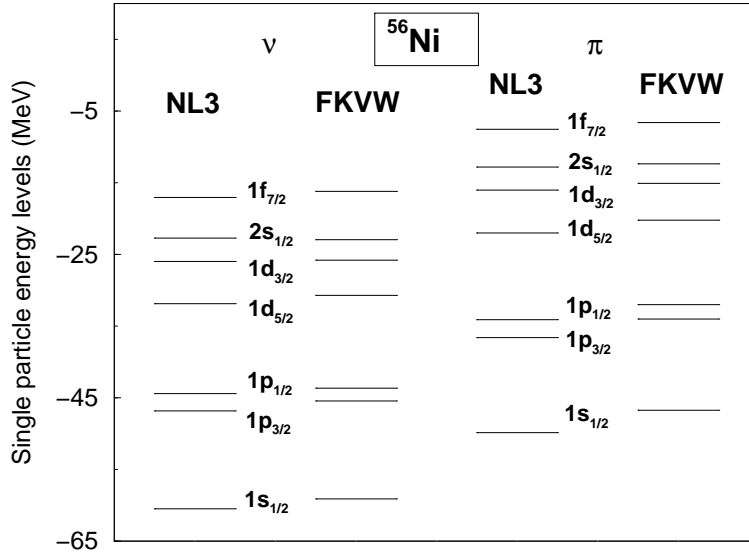


Fig. 9. Neutron and proton single-particle spectra of ^{56}Ni , calculated with the standard relativistic mean-field model NL3 effective interaction [61], and with the relativistic point-coupling model constrained by in-medium QCD sum rules and chiral perturbation theory (FKVW [13]).

model of Ref. [41]. It is also consistent with the “natural” order of magnitude expected from $D_S \sim G_S/\Lambda^2$.

The calculated neutron and proton single-particle energies of ^{16}O and ^{40}Ca are in excellent agreement with the empirical single-nucleon levels in the vicinity of the Fermi surface. In particular, with the inclusion of the isoscalar condensate self-energies, the model reproduces the empirical energy differences between spin-orbit partner states. This is an important result. It supports our primary conjecture: while nuclear binding and saturation are almost completely generated by chiral (two-pion exchange) fluctuations in our approach, strong scalar and vector fields of equal magnitude and opposite sign, induced by changes of the QCD vacuum in the presence of baryonic matter, generate the large effective spin-orbit potential in finite nuclei. Not surprisingly, the ^{40}Ca spectrum is reminiscent of an underlying pseudo-spin symmetry [60].

In Fig. 9 we compare the single-nucleon spectra of ^{56}Ni , calculated in our approach, with the results of a relativistic mean-field calculation using NL3 [61], probably the best phenomenological non-linear meson-exchange effective interaction. The agreement is convincing. All these results demonstrate that in the present approach, based on QCD sum rules and in-medium chiral perturbation theory, and with a small number of model parameters determined directly by these constraints, it is possible to describe symmetric and asymmetric nuclear matter, as well as prop-

erties of finite nuclei, at the same quantitative level as the best phenomenological relativistic mean-field models.

5.4 Systematics of binding energies and charge radii

In Table 3 we summarize our calculated binding energies per nucleon and charge radii of light and medium-heavy nuclei, in comparison with experimental values. The parameters have been kept unchanged from those used in the ^{16}O and ^{40}Ca calculations. The resulting agreement between the calculated and empirical binding energies and charge radii is indeed very good.

Table 3. Binding energies per nucleon and charge radii of light and medium-heavy nuclei, calculated in the relativistic point-coupling model constrained by in-medium QCD sum rules and chiral perturbation theory [13], are compared with experimental values.

	E/A^{exp} (MeV)	E/A (MeV)	r_c^{exp} (fm $^{-3}$)	r_c (fm $^{-3}$)
^{16}O	7.976	8.027	2.730	2.735
^{40}Ca	8.551	8.508	3.485	3.470
^{42}Ca	8.617	8.537	3.513	3.473
^{48}Ca	8.666	8.964	3.484	3.486
^{42}Ti	8.260	8.182	—	3.551
^{50}Ti	8.756	8.779	—	3.571
^{52}Cr	8.776	8.635	3.647	3.641
^{58}Ni	8.732	8.493	3.783	3.778
^{64}Ni	8.777	8.775	3.868	3.879
^{88}Sr	8.733	8.855	4.206	4.234
^{90}Zr	8.710	8.746	4.272	4.284

5.5 Density distributions

Calculated nucleon densities of ^{16}O and ^{40}Ca are plotted in Figs. 10 and 11. The results obtained in our QCD-constrained relativistic point-coupling model [13] are compared with the nucleon densities calculated in the standard relativistic mean-field meson-exchange model with the NL3 effective interaction [61]. Also shown are the corresponding charge densities in comparison with the empirical charge density profiles [62]. When compared not only with NL3, but also with other standard relativistic mean-field effective interactions, the density profiles calculated in our point-coupling model display less pronounced shell effects, in better agreement with empirical densities.

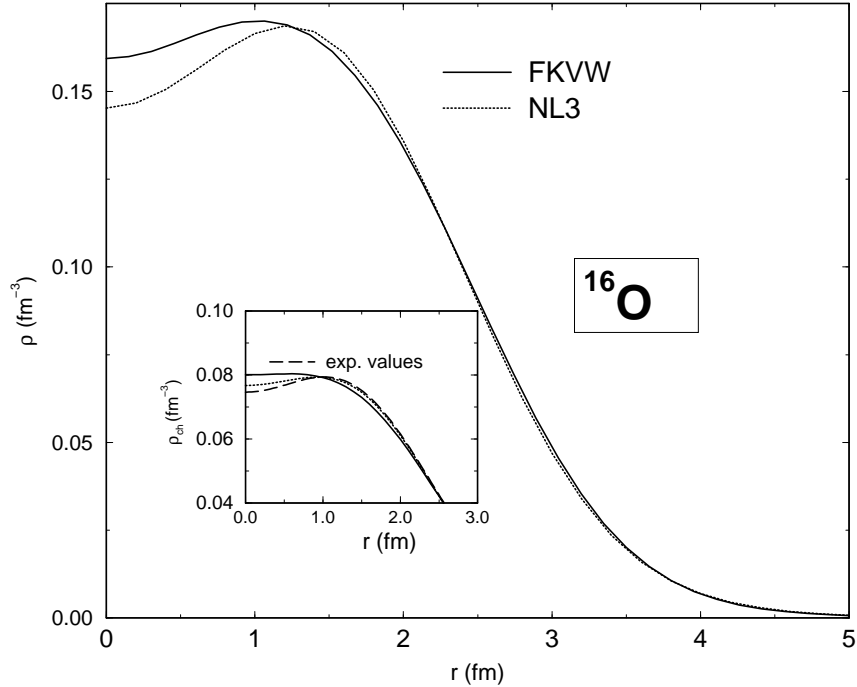


Fig. 10. Nucleon density of ^{16}O as a function of the radial coordinate. The result obtained in the QCD-constrained relativistic point-coupling model (FKVV [13]) is compared with the nucleon density calculated in the standard relativistic mean-field model with the NL3 effective interaction [61]. In the insert the corresponding charge densities are compared with the empirical charge density profile [62].

6 Concluding remarks and outlook

Our aim in these lectures notes has been to demonstrate the key role of a guiding principle, emerging from the non-perturbative dynamics of QCD: spontaneous chiral symmetry breaking. The effective field theory based on this principle ties together a wide variety of strong-interaction physics involving the lightest quarks: from the low-energy interactions of pions and nucleons via the condensate structure of the QCD vacuum and its global thermodynamical implications, to fundamental aspects of nuclear binding and saturation. Much work lies ahead; the exploration of the nuclear many-body problem in view of its low-energy QCD connections promises new insights. At the least, the QCD constraints can significantly reduce the freedom in the choice of parameters. The wide variety of results reported in previous sections have been obtained with only five parameters, two of which (the couplings $G_{S,V}^{(0)}$) turn out to be so remarkably close to leading order QCD sum rule estimates that one could have guessed their values right from the beginning. The remaining three parameters (the high-momentum scale reflecting unresolved short-distance physics,

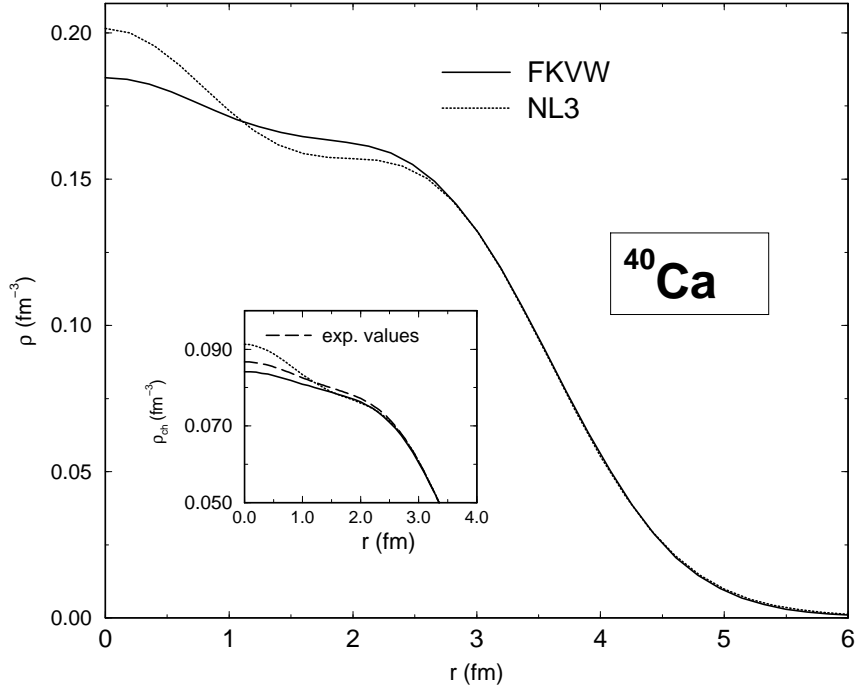


Fig. 11. Same as in Fig. 10, but for ^{40}Ca .

a "three-body" contribution to the nucleon self-energy and a surface (derivative) term) behave "naturally" according to the power-counting doctrine of effective field theory.

Of course, questions about systematic convergence of the in-medium chiral loop expansion still remain and need to be further explored. In particular, the important role of the $\Delta(1230)$, the prominent spin-isospin excitation of the nucleon, is so far just hidden in the parametrization of "short-distance" phenomena. However, the scale associated with the mass difference $M_\Delta - M_N \sim 0.3$ GeV is in fact comparable to the nuclear Fermi momentum, suggesting a more explicit treatment of the Δ in the chiral effective Lagrangian.

Calculations for heavier $N \neq Z$ nuclei are in progress. Systems such as ^{208}Pb and beyond are a test case for the detailed isospin structure of the underlying chiral pion dynamics. In the present version of the model, the isovector parts of the interaction are exclusively determined by chiral one- and two-pion exchange. Global properties of asymmetric nuclear matter and neutron matter are reproduced quite well at least at moderate densities, but pion exchange processes do not account for the short-range part of the isovector effective interaction: the resulting density dependent couplings G_{TS} and G_{TV} are presumably still too weak. There is need for stronger self-energies in the isovector channel. In meson-exchange language, such additional short-distance interactions could arise from the ρ and a_0 resonances

(where we must note, of course, that a large non-resonant low-mass part of the ρ meson channel is already accounted for by explicit isovector two-pion exchange). This is an important topic, to be further addressed in future studies which will focus on a quantitative description of heavy nuclei and extrapolations into regions of extreme isospin.

Acknowledgements

We would like to thank Norbert Kaiser whose work is at the basis of the developments reported in these notes, and Paolo Finelli and Stefan Fritsch for their contributions to this joint venture.

References

1. B.D. Serot and J.D. Walecka, *Adv. Nucl. Phys.* **16**, 1 (1986); *Int. J. Mod. Phys. E* **6**, 515 (1997).
2. P. Ring, *Prog. Part. Nucl. Phys.* **37**, 193 (1996).
3. T.E.O. Ericson and W. Weise, *Pions and Nuclei*, Clarendon Press, Oxford (1988)
4. A. Akmal and V.R. Pandharipande, *Phys. Rev. C* **56**, 2261 (1997).
5. R.J. Furnstahl and B.D. Serot, *Nucl. Phys. A* **673**, 298 (2000); *Comment. Mod. Phys.* **2**, A23 (2000).
6. T.D. Cohen, R.J. Furnstahl and D.K. Griegel, *Phys. Rev. Lett.* **67**, 961 (1991); *Phys. Rev. C* **45**, 1881 (1992).
7. E.G. Drukarev and E.M. Levin, *Nucl. Phys. A* **511**, 679 (1990); *Prog. Part. Nucl. Phys.* **27**, 77 (1991).
8. X. Jin, M. Nielsen, T.D. Cohen, R.J. Furnstahl and D.K. Griegel, *Phys. Rev. C* **49**, 464 (1994).
9. N. Kaiser, S. Fritsch, and W. Weise, *Nucl. Phys. A* **697**, 255 (2002); N. Kaiser and W. Weise, in: *The Nuclear Many-Body Problem 2001*, W. Nazarewicz and D. Vretenar, eds., Kluwer Acad. Publ. (2002); S. Fritsch, N. Kaiser and W. Weise, *Phys. Lett. B* **545**, 73 (2002).
10. N. Kaiser, S. Fritsch and W. Weise, *Nucl. Phys. A* **700**, 343 (2002).
11. N. Kaiser, S. Fritsch and W. Weise, *Nucl. Phys. A* **724**, 47 (2003).
12. P. Finelli, N. Kaiser, D. Vretenar and W. Weise, *Eur. Phys. J. A* **17**, 573 (2003).
13. P. Finelli, N. Kaiser, D. Vretenar and W. Weise, [arXiv:nucl-th/0307069], submitted to *Nucl. Phys. A*.
14. W. Weise, *Chiral Dynamics and the Hadronic Phase of QCD*, Proc. of the International School of Physics "Enrico Fermi" *From Nuclei and their Constituents to Stars*, Varenna (2002), A. Molinari et al., eds., IOS Press, Amsterdam (2003), p. 473-529.
15. A.W. Thomas and W. Weise, *The Structure of the Nucleon*, Wiley-VCH, Berlin (2001).
16. M. Gell-Mann, R. Oakes and B. Renner, *Phys. Rev.* **175**, 2195 (1968).
17. A. Pich and J. Prades, *Nucl. Phys. B Proc. Suppl.* **86**, 236 (2000).
18. B.L. Ioffe, *Phys. At. Nucl.* **66**, 30 (2003) [*Yad. Fiz.* **66**, 32 (2003)].

19. B.L. Ioffe, Nucl. Phys. **B188**, 317 (1981).
20. X. Ji, Phys. Rev. Lett. **74**, 1071 (1995).
21. J.F. Donoghue, E. Golowich and B.R. Holstein, *Dynamics of the Standard Model*, Cambridge Univ. Press (1992).
22. J. Gasser and H. Leutwyler, Ann. Phys. (N.Y.) **158**, 142 (1984).
23. S. Weinberg, Physica A **96**, 327 (1979); H. Leutwyler, Ann. Phys. (N.Y.) **235**, 165 (1994).
24. V. Bernard, N. Kaiser and U.-G. Meißner, Int. J. Mod. Phys. E **4**, 193 (1995).
25. J. Gasser, H. Leutwyler and M.E. Sainio, Phys. Lett. **B253**, 252 (1991).
26. M. Procura, T.R. Hemmert and W. Weise, [arXiv:hep-lat/0309020], subm. to Phys. Rev. D.
27. T. Schwarz, Dissertation, TU Munich (2003); W. Weise, Prog. Theor. Phys. Suppl. **149**, 1 (2003); T. Schwarz, S. Fritsch, N. Kaiser and W. Weise, work in progress.
28. A. Akmal, V.R. Pandharipande, D.G. Ravenhall, Phys. Rev. **C58**, 1804 (1998), and refs. therein.
29. R. Brockmann and R. Machleidt, Phys. Rev. **C42**, 1965 (1990), and refs. therein.
30. D.B. Kaplan, M.J. Savage and M.B. Wise, Nucl. Phys. **B534**, 329 (1998).
31. E. Epelbaum, W. Glöckle and Ulf-G. Meißner, Nucl. Phys. **A671**, 295 (2000), and refs. therein.
32. N. Kaiser, R. Brockmann and W. Weise, Nucl. Phys. **A625**, 758 (1997).
33. N. Kaiser, S. Gerstendörfer and W. Weise, Nucl. Phys. **A637**, 395 (1998).
34. R.J. Furnstahl, J.V. Steele and N. Tirfessa, Nucl. Phys. **A671**, 396 (2000).
35. H.-W. Hammer and R.J. Furnstahl, Nucl. Phys. **A678**, 277 (2000).
36. M.F.M. Lutz, B. Friman and Ch. Appel, Phys. Lett. **B474**, 7 (2000).
37. B. Friedman and V.R. Pandharipande, Nucl. Phys. **A361**, 502 (1981).
38. P.A. Seeger and W.M. Howard, Nucl. Phys. **A238**, 491 (1975).
39. B.A. Nikolaus, T. Hoch and D.G. Madland, Phys. Rev. **C46**, 1757 (1992).
40. J.J. Rusnak and R.J. Furnstahl, Nucl. Phys. **A627**, 495 (1997).
41. T. Bürvenich, D.G. Madland, J.A. Maruhn and P.G. Reinhard, Phys. Rev. **C65**, 044308 (2002).
42. R.J. Furnstahl, H.-B. Tang, and B.D. Serot, Phys. Rev. **C52**, 1368 (1995).
43. R.J. Furnstahl and B.D. Serot, Nucl. Phys. **A671**, 447 (2000).
44. A. Manohar and H. Georgi, Nucl. Phys. **B234**, 189 (1984).
45. J.L. Friar, D.G. Madland and B.W. Lynn, Phys. Rev. **C53**, 3085 (1996).
46. P. Manakos and T. Mannel, Z. Phys. **A334**, 481 (1989).
47. C. Fuchs, H. Lenske, and H.H. Wolter, Phys. Rev. **C52**, 3043 (1995).
48. F. de Jong and H. Lenske, Phys. Rev. **C57**, 3099 (1998).
49. F. Hofmann, C.M. Keil and H. Lenske, Phys. Rev. **C64**, 034314 (2001).
50. S. Typel and H.H. Wolter, Nucl. Phys. **A656**, 331 (1999).
51. T. Nikšić, D. Vretenar, P. Finelli and P. Ring, Phys. Rev. **C66**, 024306 (2002).
52. T. Gross-Boelting, C. Fuchs and A. Faessler, Nucl. Phys. **A648**, 105 (1999).
53. S.K. Bogner, T.T.S. Kuo and A. Schwenk, [arXiv:nucl-th/0305035]; A. Schwenk, G.E. Brown and B. Friman, Nucl. Phys. **A703**, 745 (2002).
54. W. Kohn and L. J. Sham, Phys. Rev. **140**, A1133 (1965).
55. W. Kohn, Rev. Mod. Phys. **71**, 1253 (1999).
56. R. M. Dreizler and E. K. U. Gross, *Density Functional Theory*, Springer, Heidelberg, 1990.

57. Y.K. Gambhir, P. Ring and A. Thimet, *Ann. Phys. (N.Y.)* **198**, 132 (1990).
58. B.D. Serot and J.D. Walecka, *Phys. Lett.* **B87**, 172 (1979).
59. R. Brockmann and W. Weise, *Phys. Rev.* **C16**, 1282 (1977).
60. J.N. Ginocchio, *Phys. Rev.* **C66**, 064312 (2002).
61. G.A. Lalazissis, J. König, and P. Ring, *Phys. Rev.* **C55**, 540 (1997).
62. H. de Vries, C.W. de Jager, and C. de Vries, *At. Data Nucl. Data Tables* **36**, 495 (1987).